Uppsala. 1961

ARKIV FÖR KEMI

UTGIVET AV

KUNGL. SVENSKA VETENSKAPSAKADEMIEN

Band 18 nr 1

GUNNAR WETTERMARK

High intensity photolysis studies of acetone and some aliphatic aldehydes

---

ALMQVIST & WIKSELL

STOCKHOLM

GÖTEBORG · UPPSALA

1961

R. UNIV.
BIBLIOTHEEK
LEIDEN

HIGH INTENSITY PHOTOLYSIS STUDIES OF ACETONE AND SOME ALIPHATIC ALDEHYDES

INAUGURAL DISSERTATION

by

GUNNAR WETTERMARK

FIL. LIC., KALM.

BY DUE PERMISSION OF THE FACULTY OF SCIENCE
OF THE UNIVERSITY OF UPPSALA
TO BE PUBLICLY DISCUSSED IN THE LECTURE HALL
OF THE INSTITUTE OF CHEMISTRY ON MAY 23, 1961,
AT 10 A.M.,
FOR THE DEGREE OF DOCTOR OF PHILOSOPHY

*

The discussion with the Opponent of the Faculty will be in English

UPPSALA 1961

ALMQVIST & WIKSELLS BOKTRYCKERI AB

R. UNIV.
BIBLIOTHEEK
LEIDEN

ARKIV FÖR KEMI Band 18 nr 1

Communicated 12 April 1961 by T. Svedberg and A. Fredga

High intensity photolysis studies of acetone and some aliphatic aldehydes

By Gunnar Wettermark

With 28 figures in the text

CONTENTS

Introduction 1
Section 1. *Methods* 3
General procedure 3
Photolysis in Apparatus II 4
Determination of quantum yields with Apparatus III 5
Gas chromatography 17
Chemicals 20
Section 2. *General theory* 21
Section 3. *Results and discussion* 27
General presentation and consideration 27
Acetone 29
Acetaldehyde 45
Propionaldehyde 51
n-Butyraldehyde 57
Isobutyraldehyde 62
Aldehydes (Reactions which are first order with respect to radical concentration. Quantum yields) 65
Summary 73
Acknowledgements 77
References 77

Introduction

A considerable amount of knowledge about the reactions of free radicals and electronically-excited molecules has arisen from the study of the products of systems photolyzed with low light intensities of the order of 10^{15} quanta sec^{-1} $litre^{-1}$. In this connection, particular attention has been paid to the vapour phase photolysis of acetone and the simple aliphatic aldehydes. It has been shown that this photolysis occurs to a great extent by a free radical mechanism. Extensive reviews of the subject have been published, but the detailed mechanism is still a matter of controversy [1, 2, 3, 4].

Recent work has shown, however, that a striking simplification of the reaction scheme can be obtained with the use of a high intensity light source such as a flash

lamp. Under these circumstances, very high concentrations of electronically-excited molecules and free radicals are generated. Reactions between radicals and parent molecules can then usually be eliminated in view of the high efficiency of the radical–radical reactions. Thus, in particular, high intensity work provides information about the primary photochemical steps.

The high intensity photolysis of acetone and acetaldehyde has been studied with a gas discharge lamp by Khan, Norrish and Porter [5]. Using a spiral lamp wound around the reaction vessel, they subjected the sample to absorbed intensities of the order of 10^{24} quanta sec^{-1} $litre^{-1}$, the duration of the flash being 150 μsec. These workers found that the results of their studies were essentially in agreement with those obtained using low light intensities.

Mains, Roebber and Rollefson used a spark apparatus with an intensity of about 10^{22} quanta sec^{-1} $litre^{-1}$ for a brief study of the photolysis of acetaldehyde [6]. In this work, a capacitance of 10 μF and 20 kV was discharged between ten pairs of magnesium electrodes in a low pressure chamber at the centre of which the reaction vessel was placed. The spark was reported to give monochromatic light at 280 mμ due to an intense group of magnesium lines, about 90 % of the light measured with a ferrioxalate actinometer being attributed to these lines. With this apparatus, and using flash times of 140 and 2400 μsec, a more extensive investigation of the photolysis of acetone was undertaken by Roebber, Rollefson and Pimentel [7]. On the basis of their results, they proposed a modification of the previously accepted mechanism.

Using an exploding wire as a light source, Oster and Marcus investigated the high intensity photolysis of acetone [8, 9]. In this case, a cylindrical quartz reaction vessel was arranged parallel to the exploding wire and the flash period amounted to 300 μsec. In some of the experiments, a cylindrical cellophane filter was employed which absorbed most of the light below 210 mμ. Some of the findings from this work are contradictory to the results of Roebber, Rollefson and Pimentel.

The present work represents a more detailed study of the high intensity photolysis of acetone and acetaldehyde. The high intensity photolysis of propionaldehyde, *n*-butyraldehyde and isobutyraldehyde has also been investigated in detail. By using new techniques, it was hoped that this study would provide further information about the reactions of the electronically-excited molecules and free radicals involved.

There are certain factors which must be taken into account in order to derive useful information from the flash photolysis experiments.

One of the factors is the desirability of exposing the sample to one single flash. In order to obtain high concentrations of electronically-excited molecules and free radicals, this flash should be short and of high energy. The products formed in the initial stages of the photolysis may affect the reaction pattern in the further photolysis, and can then introduce complications in the interpretation of the results [8, 10]. These complications can be expected to be of a more serious nature when several flashes are used. With most of the flash lamps which have been constructed, the amount of products formed in a single flash will be too small for quantitative analysis using the available analytical techniques.

If large doses are supplied in a single flash, adiabatic heat effects will result in a drastic temperature rise. This temperature change can be reduced by increasing the heat capacity of the system through the addition of large amounts of inert gas. In this case, one must be careful when interpreting the data to ensure that the effects of any foreign molecules on the primary process are taken into consideration.

A problem is that the discharge is usually a source of highly polychromatic light. Ideally the incident light should be monochromatic, but any attempt to monochromatize it results in most cases in an undue loss of intensity.

The kinetics will be seriously complicated if the degree of excitation is not homogeneous throughout the reaction vessel. This means that the absorption of the sample must be kept low.

Quantum yields will be very difficult to evaluate unless the light beam is parallel. As a very small part of the light emitted from the flash lamp is used in such work with parallel light, extremely intense light sources are needed.

The interpretation of the results from measurement of the ratios between the amounts of some of the products formed can easily result in misleading information. In very few of the investigations undertaken into the photolysis of acetone and the simple aliphatic aldehydes has an attempt been made to measure all the products formed and to make a complete mass balance calculation of the products. Experiments where even the minor components amongst the products are measured certainly provide better information about the nature of the processes involved.

Section 1. Methods

General procedure

The present investigation was made possible by the development of very intense flash light sources of short flash duration, which has been proceeding at this Institute for the last ten years [11, 12, 13]. A large number of different types of apparatus has been constructed to meet the various requirements of studies using the flash photolysis method. By employing two of the five flash photolysis units which are now in operation, the difficulties described in the introduction were met in the following way.

An analysis for most of the formed products was made on samples which were exposed to unfiltered light. In this part of the investigation, the substances were photolyzed in cylindrical reaction vessels in a flash photolysis apparatus giving a very short pulse of light with high intensity (Apparatus II). The flash duration of this apparatus is about 10 μsec. It was thought that with this apparatus high concentrations of electronically-excited molecules and free radicals could be generated without feeding too much energy into the system. To measure the influence of temperature, large amounts of helium were added in some experiments. Gas chromatographic analysis for the products was undertaken using a high sensitivity thermal conductivity detector or a flame ionization detector. The results show that most of the products formed in the photolysis could be measured in this way.

By using a very intense point-discharge it has been possible to make quantum yield determinations in parallel light (Apparatus III). About 10^{22} quanta of "chemically active light" are given off at the discharge, "chemically active light" being defined as light measured with the ferrioxalate actinometer. A small spherical angle of the discharge is used, and parallel light is obtained by a set of diaphragms. Although the number of quanta given off in each flash is considerable, that number reaching the reaction vessel is comparatively low. The absorption of the sample is kept low, the number of quanta absorbed in a reaction vessel which has a volume of about 1.3 ml being less than 10^{17} quanta. In all cases, the samples have been subjected to one single flash. The amount of products has been measured by means of gas chro-

matography using a flame ionization detector. By the use of this method, it has been possible to make analysis of products in amounts as small as 10^{-9} g. Due to the limitations mentioned above (small spherical angle and low absorption), it is necessary to irradiate the samples over a comparatively broad wavelength region to achieve a suitable decomposition. The samples absorb light in the wavelength band around 280 mμ, the low wavelength limit being set by a cut-off filter and the long wavelength limit by the transmission of the sample itself. About 0.5 % of the molecules absorb a quantum. The energy put into the system is considerable and the temperature rise will thus be high. In order to determine the influence of temperature, helium was added in some experiments. As about 0.01 % of the substance is photolyzed, it has only been possible to obtain quantum yields for the main products. The quantum yields were determined at different pressures of the parent substance. As mentioned in the introduction, the photolyzed substances are acetone, acetaldehyde, propionaldehyde, *n*-butyraldehyde and isobutyraldehyde. For the different substances, the products measured are as follows:

acetone–ethane;
acetaldehyde–methane and ethane;
propionaldehyde–ethane;
n-butyraldehyde–propane and ethylene;
isobutyraldehyde–propane.

Photolysis in Apparatus II

Apparatus II was constructed by Claesson and Lindqvist [12]. In this apparatus, the discharge is of very short duration and takes place in an annular compartment outside a transparent quartz lamp tube. The reaction vessel is placed inside this tube. In the present investigation the lamp was used with iron electrodes. Owing to darkening of the lamp tube, the intensity decreases strongly during the first flashes. After a few hundred flashes the dose given off in each flash takes on a constant value and the lamp can then be used without further reduction of the intensity. The spectrum emitted from the flash lamp is continuous, with superimposed lines, and is rather constant throughout the quartz ultraviolet and visible regions. The low wavelength limit is set by the absorption of the quartz.

In the present investigation, the lamp was used at a constant voltage (5 kV) and with a constant capacity (144 μF). In this way, it is ensured that the spectral distribution of the light emitted from the lamp remains constant. The apparatus has a very low inductance, a flash duration of 10 μsec being achieved at the voltage and capacity given above. The duration of the flash is defined as the time interval from $1/e$ of maximum light intensity on the rising part of the curve to the corresponding point on the descending part. The flash profile was obtained by recording unfiltered light with a phototube (RCA 935) and oscilloscope.

Reaction vessels for use with Apparatus II are seen in Fig. 1. Each vessel consists of a cylindrical quartz tube (inner diam. 11.5 mm) which is connected to a stopcock by means of a ground joint. Only the outer part of this joint is greased. The cell is designed in such a way that the contact between the sample and the grease is kept to a minimum. The reaction vessel which was used in the study of the photolysis of acetone had a volume of 9.16 ml. In the rest of the investigation work, two cells were employed, having volumes of 6.12 and 6.14 ml.

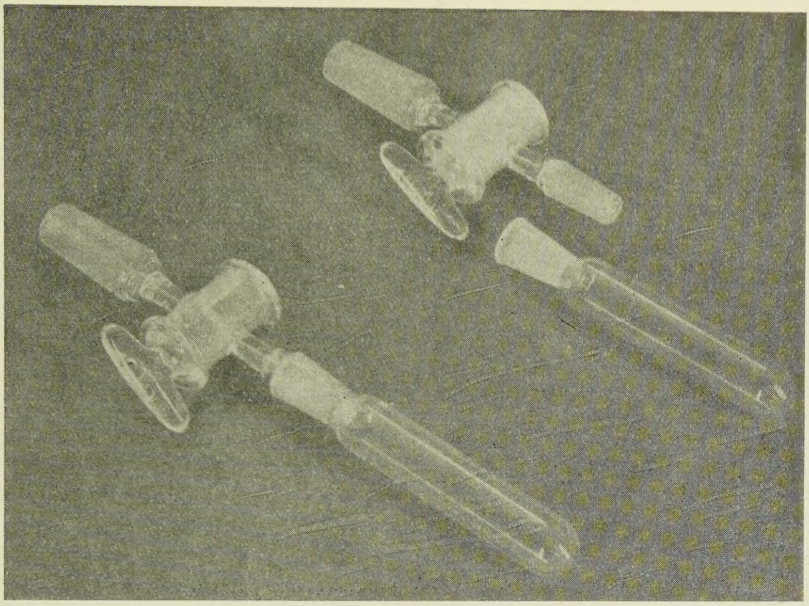

Fig. 1. Reaction vessels for use with Apparatus II. Each vessel has an inner diameter of 11.5 mm.

The light output was frequently checked by means of chemical actinometry. A uranyl oxalate actinometer was used, the solution containing 0.001 *M* uranyl oxalate and 0.004 *M* oxalic acid. The reaction vessel was filled with the actinometer solution, and after exposure titrations were made with ceric sulphate as described by Claesson and Lindqvist [11]. The light output measured in this way showed a maximum variation of 4 % from the mean value for the determinations. Using an average value of 0.6 for the quantum yield, the light absorbed by the uranyl oxalate actinometer was calculated to be 3.2×10^{18} quanta in the acetone work and 2.4×10^{18} quanta in the work with the aldehydes. This corresponds to an intensity of 4×10^{25} quanta sec^{-1} $litre^{-1}$. Much higher intensities can be gained with this lamp if it is cleaned between the flashes. This was not necessary for the present investigations, however.

In all cases the sample has been subjected to one single flash at room temperature ($23 \pm 2°C$) and immediately transferred to the gas chromatograph for analysis.

Determination of quantum yields with Apparatus III

Experimental arrangements

Apparatus III is a flash photolysis apparatus with energies up to about 400,000 joules. It will be described in a separate paper and only some brief data will be given here [14].

The condensor bank consists of 504 units. Each of these units has a capacity of about 2 μF and can be charged to a voltage of about 30 kV. The total capacity thus amounts to about 1000 μF. The condensors are mounted in two symmetrical halves, one half being charged to a positive potential and the other half to a negative poten-

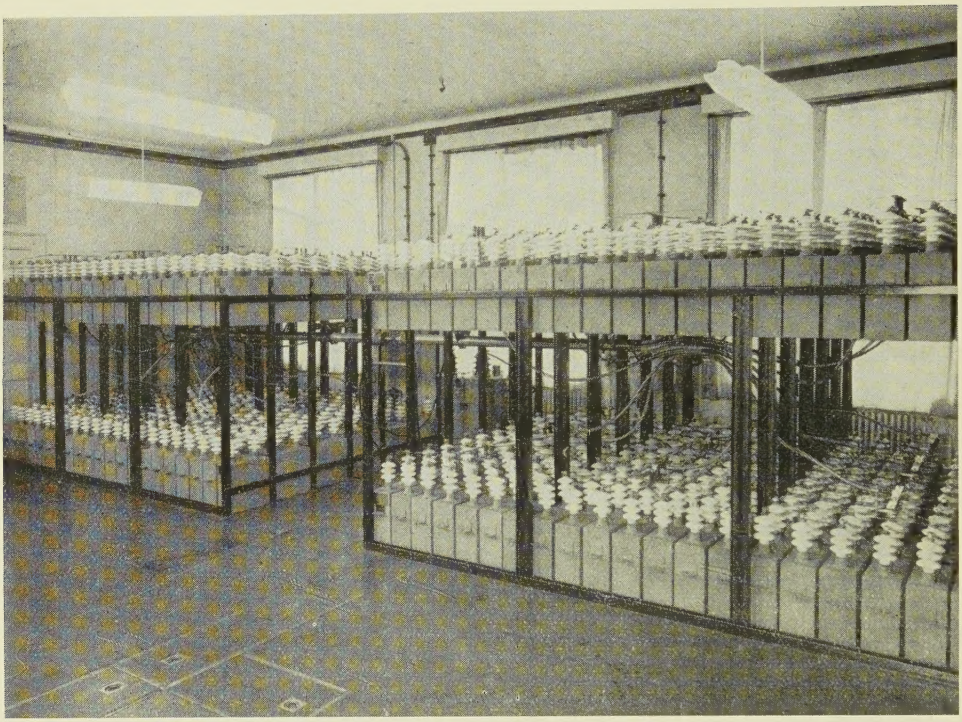

Fig. 2. The large flash photolysis apparatus (Apparatus III). The maximum energy stored is 400,000 joules.

tial. Each half contains 18 groups with 14 condensors connected in parallel, and the groups are connected to the lamp through coaxial cables. The halves are arranged in two planes. Fig. 2 gives a total view of the apparatus.

In the present investigation, the condensor bank was discharged in the air between two conical brass electrodes. The lamp construction is shown in Fig. 3. Photographs of the discharge show that it is almost spherical with a diameter of about 30 mm. The present work has been undertaken using a constant energy of 100,000 joules. The condensor bank was charged to the desired voltage (14.2 kV) keeping the electrodes sufficiently apart so that the apparatus did not fire spontaneously. The discharge was then started by blowing a stream of argon axially through the spark gap through a central hole. The rubber tube in Fig. 3 is the inlet for the argon stream. The light dose given off at a discharge is found to be dependent on the electrode distance, which was kept constant at 22 mm.

A special technique was developed in order to keep the incident light parallel. A sector shaped holder for five reaction vessels was designed in such a way that all the five reaction vessels "see" approximately the same part of the discharge (Figs. 4 and 5). The holder is made of polyvinyl plastic with five cylindrical channels, the axes of which intersect at a point, and is fixed to an optical bench so that this point of intersection and the centre of the discharge coincide. Four blackened dia-

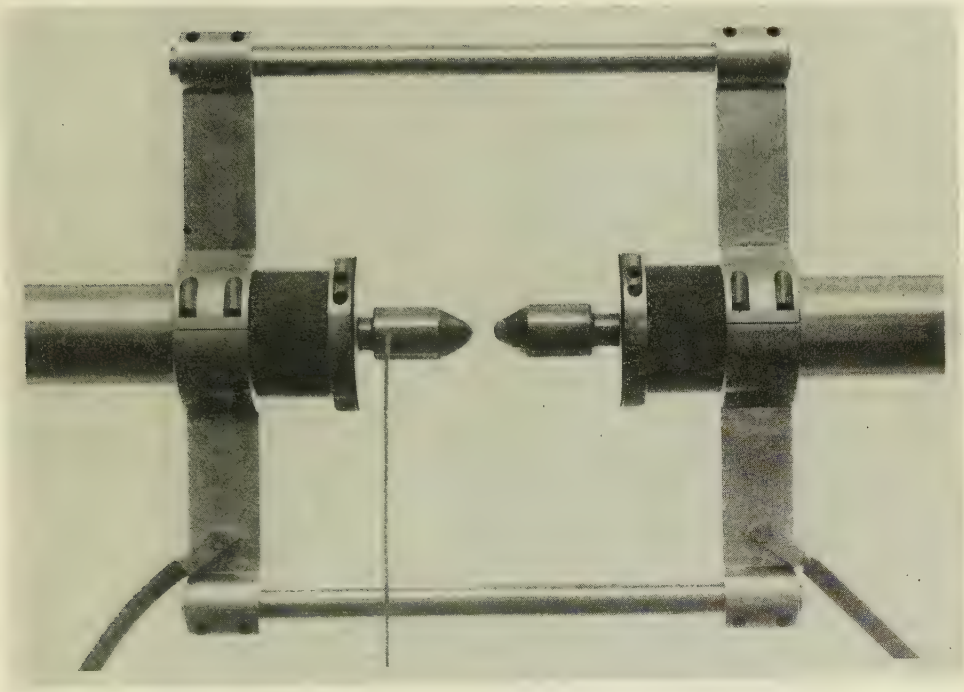

Fig. 3. The spark gap used for the point-discharge of Apparatus III.

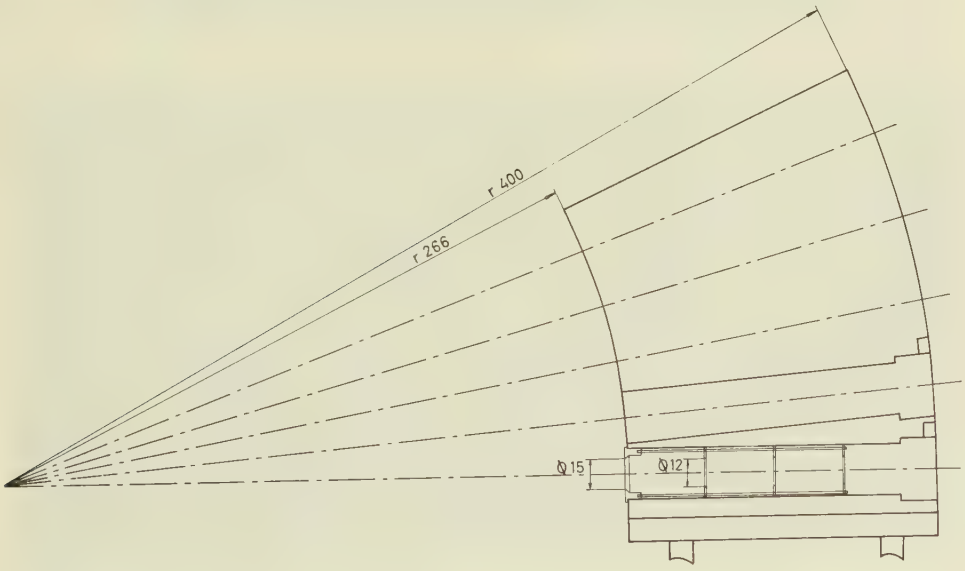

Fig. 4. The sector shaped holder for use together with Apparatus III. All units are given in mm.

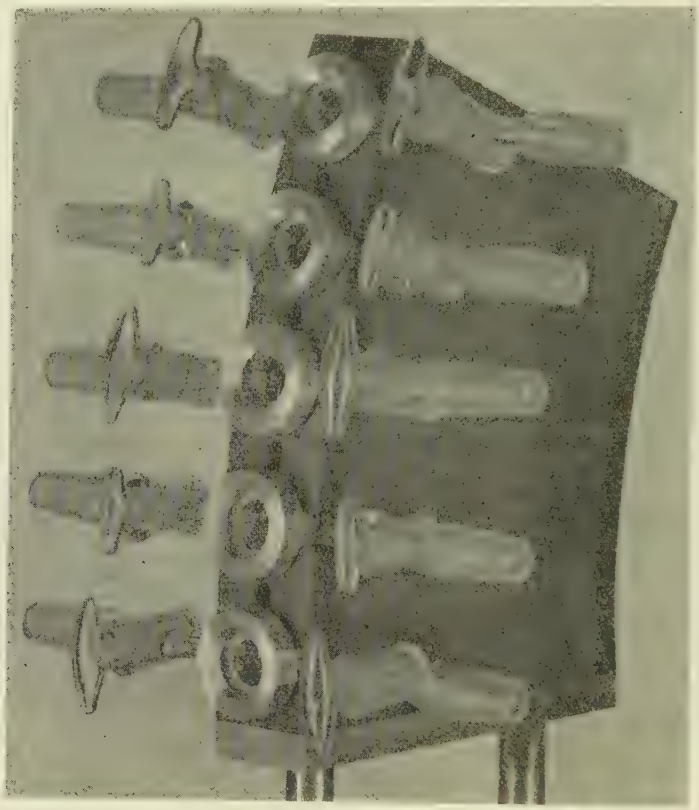

Fig. 5. Photograph of the sector shaped holder with the reaction vessels.

Fig. 6. Reaction vessels for use together with Apparatus III. The volume of each vessel is 1.3 ml.

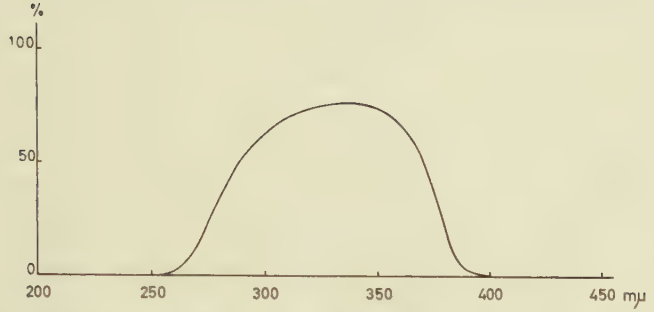

Fig. 7. The transmittance of the filter employed in the irradiations with Apparatus III (Jena UG 11, 2 mm).

phragms are placed in the channels in such a way that they limit the aperture and make the incident light almost parallel.

Fig. 6 shows the construction of the reaction vessel. The centre piece, which has a cylindrical cross section, is made of glass with two stopcocks. The slight divergence of the light beam is compensated for by making the central piece of the reaction vessel conical with the same angle as the light beam. In this way, all incident light passes into the sample and none is reflected from or absorbed by the walls. The optical depth of the vessel is 10 mm. Contact between the sample and the stopcock grease is kept to a minimum by the use of 1 mm capillaries whose dead volume is small, amounting to about 0.04 ml. The reaction vessel is provided with plane parallel quartz windows, the front window in the present experiments being replaced by a filter (Jena UG 11, 2 mm) whose transmittance is given in Fig. 7. The filter and the end window were cemented to the cylindrical centre portion with araldite. It is seen from the figure that the vessel is placed into a housing of aluminium, which provides diaphragms in front and at the back (diams. 11 and 16 mm). The spherical angle formed is the same as for the centre piece and it is thus ensured that none of the light transmitted can be reflected back from the end diaphragm. The volume of each of the five reaction vessels is about 1.3 ml, the maximum difference in volume between any two vessels being 0.06 ml.

The number of quanta falling into each reaction vessel was measured by means of chemical actinometry using potassium ferrioxalate as actinometer substance. It was

Table 1. The number of quanta absorbed in each of the five reaction vessels by a 0.006 *M* ferrioxalate actinometer. The values from three consecutive flashes are shown (Apparatus III, 100,000 joules, filter Jena UG 11, 2 mm).

Reaction vessel	Flash I quanta $\times 10^{-17}$	Flash II quanta $\times 10^{-17}$	Flash III quanta $\times 10^{-17}$
1	6.03	5.44	6.23
2	6.13	5.53	6.18
3	6.08	5.41	6.27
4	6.01	5.36	6.15
5	6.18	5.36	6.08
Mean value	6.09	5.42	6.18

Fig. 8. The spectral distribution of the light incident on the reaction vessels from the point-discharge of Apparatus III (100,000 joules).

found that all the reaction vessels received the same number of quanta for each flash within the limits of experimental error. Table 1 shows the number of quanta absorbed in each reaction vessel for each of three consecutive flashes. The values are calculated using an average value of 1.2 for the quantum yield. The concentration of the actinometer solution was 0.006 M and the actinometer was used exactly as described by Hatchard and Parker [15].

When the photolysis of acetone and the aldehydes was being investigated, five reaction vessels were irradiated simultaneously, a 0.006 M ferrioxalate solution being kept in two of the vessels. All measurements were made at room temperature (23 $\pm$ 2°C). The vessels were exposed to one single flash and the decomposition of the actinometer (the amount of Fe^{2+} ions produced) was determined according to the instructions given by Hatchard and Parker [15]. The other reaction vessels were immediately transferred to the gas chromatograph for analysis.

Determination of the absorbed dose

The light dose received by the sample was calculated from the decomposition of the actinometer. The following quantities have to be determined as a function of wavelength, λ, in order to make these calculations possible.

1. The number of quanta emitted from the flash in the wavelength region λ to $\lambda + d\lambda$, $S(\lambda)d\lambda$. 2. The transmittance of the filter, $T(\lambda)$. 3. The quantum yield of decomposition of the actinometer, $\phi(\lambda)$. 4. The fraction of the light incident on the sample which is absorbed by the sample, $A_1(\lambda)$. 5. The fraction of the light incident on the actinometer which is absorbed by the actinometer, $A_2(\lambda)$.

$A_1(\lambda)$ and $A_2(\lambda)$ refer to the optical depth of the reaction vessel. No correction for the slight divergence of the light beam in the reaction vessel is applied. The approximation made is, however, small.

1. A considerable amount of work was devoted to obtaining the spectral distribution of the light emitted from the flash. These measurements were made with a

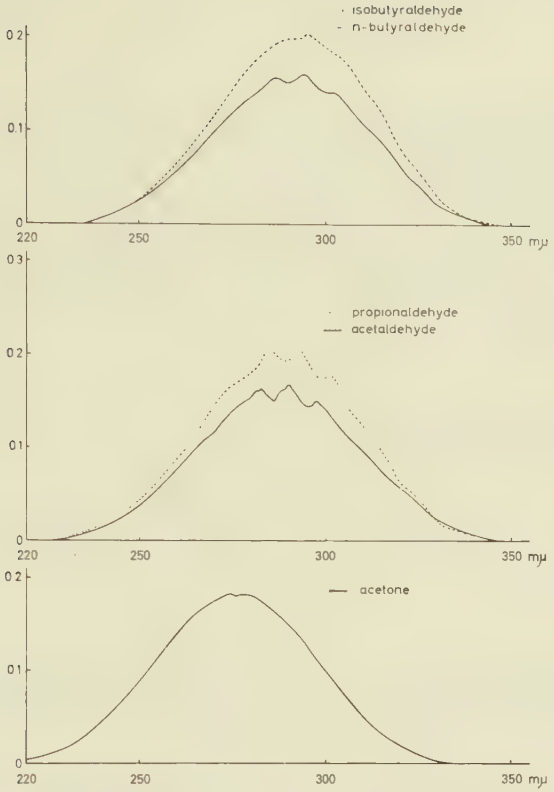

Fig. 9. Optical density curves $[\log_{10}(I_0/I)]$ for five cm layers of acetone (50.2 mm Hg), acetaldehyde (50.0 mm Hg), propionaldehyde (50.7 mm Hg), *n*-butyraldehyde (50.1 mm Hg), isobutyraldehyde (50.2 mm Hg).

monochromator and a vacuum phototube connected to an oscilloscope. The determination involved, besides the actual measurements on the flash, a set of calibrations of the units employed in the recording of the spectrum and is described in a separate paragraph. The final curve $S(\lambda)$ is shown in Fig. 8.

2. $T(\lambda)$ was determined in a Beckman DU spectrophotometer.

3. Using the values given by Hatchard and Parker, the quantum yield plotted versus wavelength gives the desired function $\phi(\lambda)$. It is shown in reference [16]. It is believed that the use of normal quantum yields at these high intensities involves no approximation [11].

4. Beer's law can be written in the form

$$\log_{10} \frac{I}{I_0} = -\varepsilon [S] l, \qquad \{1\}$$

where I_0 is the intensity of the incident light, I that of the transmitted, ε the extinction coefficient, $[S]$ the concentration and l the thickness of the layer that the light has passed. The fraction of the light incident on the sample which is absorbed by the sample is thus

$$A = \frac{I_0 - I}{I_0} = 1 - 10^{-\varepsilon[S]l}. \qquad \{2\}$$

In the present investigation the value $\varepsilon[S]l$ for the sample was determined as a function of wavelength for a set of pressures and $A_1(\lambda)$ calculated by means of Eq. {2} for these pressures. The determinations of $\varepsilon[S]$ were made in a manual Zeiss spectrophotometer PMQ 11. As the absorption coefficients are low, cuvettes with an optical depth of 5.00 cm were used. Fig. 9 shows the measurements of $\log_{10}(I_0/I)$ as a function of wavelength for five cm layers of acetone, acetaldehyde, propionaldehyde, *n*-butyraldehyde and isobutyraldehyde at about 50 mm Hg pressure.

In the pressure interval investigated, $\varepsilon[S]$ was shown to be proportional to the pressure of the substance,

$$\varepsilon[S] = \alpha p, \qquad \{3\}$$

α being a constant and p the pressure.

The absorbed intensity, I_a, is thus given as

$$I_a = I_0 - I = I_0(1 - 10^{-\alpha p l}). \qquad \{4\}$$

At low pressures, the higher order terms in the Maclaurin's series can be neglected and one thus obtains

$$I_a = (\ln 10)\,\alpha p l I_0. \qquad \{5\}$$

5. $A_2(\lambda)$ was calculated by means of Eqs. {1} and {2} from measurements in a Beckman DU spectrophotometer. The curve is shown in reference [16].

The number of quanta absorbed by the sample is given by the equation

$$Q = \beta \int S(\lambda)\, T(\lambda)\, A_1(\lambda)\, d\lambda, \qquad \{6\}$$

where β is a constant. The number of molecules decomposed (amount of Fe^{2+} ions produced) in the actinometer is

$$N = \beta \int S(\lambda)\, T(\lambda)\, A_2(\lambda)\, \phi(\lambda)\, d\lambda. \qquad \{7\}$$

The ratio between the number of quanta absorbed by the sample and the number of molecules decomposed in the actinometer is thus

$$\frac{Q}{N} = \frac{\int S(\lambda)\, T(\lambda)\, A_1(\lambda)\, d\lambda}{\int S(\lambda)\, T(\lambda)\, A_2(\lambda)\, \phi(\lambda)\, d\lambda}. \qquad \{8\}$$

For the various experimentally determined $A_1(\lambda)$ curves, the quantity Q/N was calculated by graphical integration. For the different substances, plots of Q/N versus pressure were drawn, thus making it possible to determine the value of Q/N at any pressure. In all experiments, the light dose absorbed by the sample has been calculated by multiplying the value of Q/N, obtained from these graphs, by the number of molecules decomposed in the actinometer. The latter quantity was calculated from the mean value of the decomposition measured in the two reaction vessels containing actinometer solution.

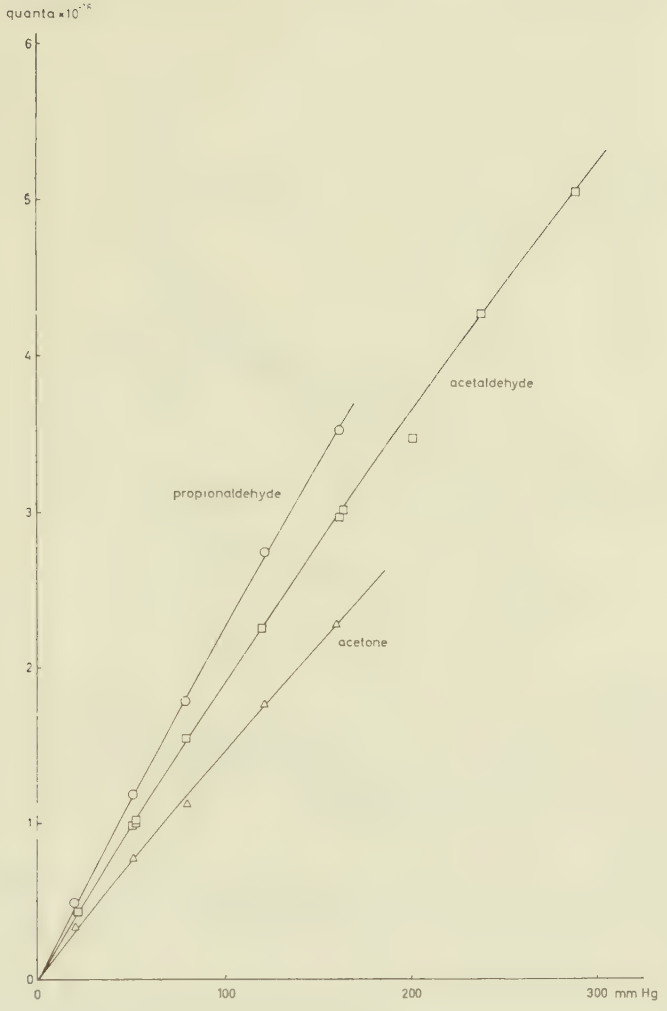

Fig. 10. The number of quanta absorbed by the sample in the reaction vessel as a function of the pressure of the sample.

The quantity of light absorbed from each flash is thus directly measured by actinometer decomposition in every case. This is of importance, as the doses emitted by a series of flashes vary, and the use of a mean value for the flash dose will therefore result in some error.

A mean value for β can be determined from the spectral distribution, as all calibrations involved were made in absolute units. Another value for β was also obtained from a mean of all the actinometric experiments. Comparison of the two values showed that the former was about 25 % lower than the latter. It is to be expected that the former value would be somewhat erratic as several steps with a rather low degree of accuracy are involved in the absolute calibration.

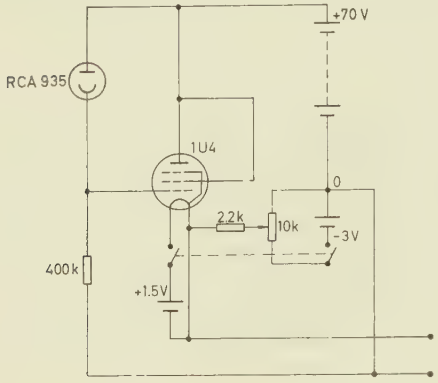

Fig. 11. Circuit diagram for the photocell with the cathode follower.

The number of quanta absorbed by the sample is given as a function of pressure in Fig. 10 for acetone, acetaldehyde and propionaldehyde. The absorbed dose is calculated by means of Eq. {6}, using the value of β obtained from the spectral distribution curve.

Determination of the spectral distribution of the light emitted from the point-discharge of Apparatus III

The spectral distribution of the light from Apparatus III was obtained by the use of a monochromator, a vacuum photocell and an oscilloscope. The determination involved, besides the actual measurements on the flash, a set of calibrations of the units employed in the recording of the spectrum. These calibrations consisted in the determination of the dispersion and transmission of the monochromator, together with the derivation of the spectral sensitivity of the phototube. The following steps were undertaken.

1. The monochromator was placed with the entrance slit at the position of the reaction vessel behind the sector shaped holder. At the exit slit, a phototube and a cathode follower were mounted in a well-shielded box and the signal read on an oscilloscope. The oscilloscope curve of light intensity versus time was photographed with the monochromator set at different wavelengths. 71 recordings were made to cover the wavelength region 200 to 600 mμ. To apply a correction for the variation in the amount of light emitted from different flashes, another phototube simultaneously recorded the entire spectrum for each flash.

The monochromator was a quartz prism instrument (Zeiss Spiegel monochromator). The slit widths of the monochromator were kept constant at 0.25 mm for both entrance and exit slits, a narrow spectral region, amounting to 12 mμ when widest (at 600 mμ), thus being isolated. It was found most suitable to have the photocell (RCA 935) directly connected to the monochromator, although a current of the order of 100,000 A was raised simultaneously only 80 cm away. In this way, calibration of optical parts behind the monochromator, which might otherwise make the results less accurate, was avoided. Thus only the photocell had to be calibrated. On the other hand, the phototube had to be particularly well shielded. It was found necessary to have a cathode follower directly connected to the photocell, the circuit diagram being shown in Fig. 11. The 70 V potential was drawn from small batteries

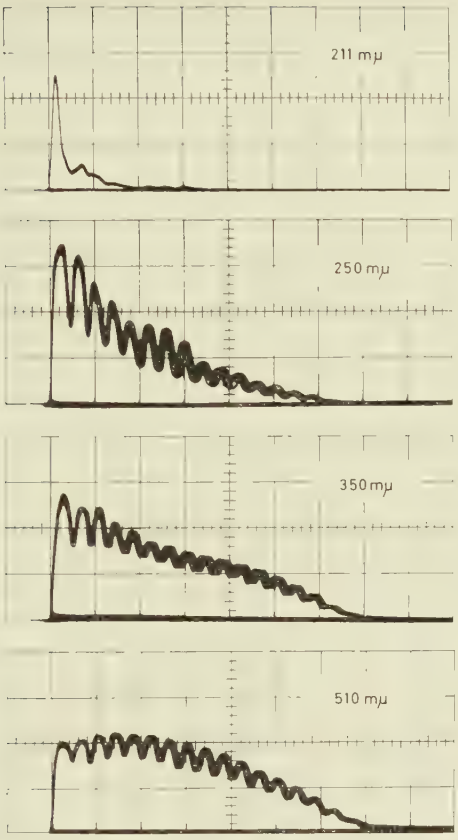

Fig. 12. Oscillograms of light intensity as a function of time for the point-discharge of Apparatus III (100,000 joules). In the four curves different wavelengths of the emitted light have been isolated. One scale division corresponds to 100 μsec.

used for various types of photographic flash apparatus. The entire unit was mounted in a small box consisting of four layers of soft iron and two layers of aluminium. It had a time constant of 2 μsec, which was sufficient for these measurements. The signal was read on a Tektronix 541 oscilloscope. Another identical system with phototube and oscilloscope but without monochromator, recorded the entire spectrum.

2. The dispersion of the monochromator was determined by using some spectral lines from Philips discharge lamps.

3. The transmission of the monochromator was measured as a function of wavelength by determining the intensity of a monochromatic light beam before and after passing the monochromator. These measurements were made with the manual Zeiss spectrophotometer PMQ 11. Care was taken to ensure that the monochromator had the same aperture in these determinations as during the measurements on the flash.

4. In the calibration of the photocell, a chemical actinometer and a bolometer were employed. The actinometer was 0.006 *M* potassium ferrioxalate which was used in

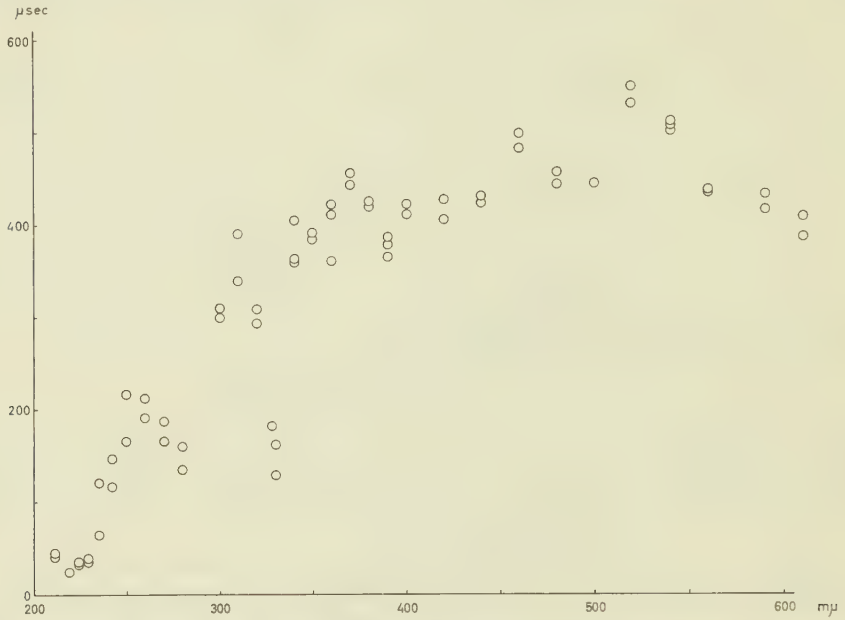

Fig. 13. The flash duration as a function of wavelength for the point-discharge of Apparatus III (100,000 joules).

exact accordance with the instructions given by Hatchard and Parker [15]. The bolometer is a commercial instrument manufactured by Ing. H. Röhrig, Berlin-Steglitz. The spectral sensitivity was determined in absolute units at a few wavelengths by the help of the actinometer, and the bolometer made it possible to obtain values for the entire wavelength region. To reach intensities of light comparable to those obtained during the measurement on the flash, an intense light source had to be used (Philips SP 500 W). At a few wavelengths it was possible to use a monochromator. The spectral sensitivity curve is known, however, to be smooth enough to make it possible to use a set of interference filters to isolate different wavelength regions for these calibrations. Interference filters were thus combined with Jena absorption filters to isolate different bands in the spectrum of the lamp. A set of 12 interference filters was used to cover the region 250–600 mμ (Barr and Straud, Bausch and Lomb). The spectral sensitivity curve obtained for the phototube was found to agree closely with the curve given by the manufacturer.

Some oscillograms at a few wavelengths are shown in Fig. 12. The flash profile and the duration of the flash are strongly dependent on the wavelength. Fig. 13 shows the variation of the flash duration with wavelength in the interval 200–600 mμ. The duration is measured at $\frac{1}{2}$ of peak intensity on a smoothened curve, each point representing the measurement on one single flash. To make a correction for the variation in the dose given off in different flashes, the flash durations given in the figure have been normalized with the help of the oscillograms from the photocell recording the entire spectrum. The times given in Fig. 13 are thus obtained in each

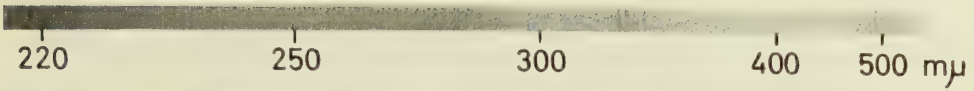

Fig. 14. The emission spectrum of the point-discharge of Apparatus III (100,000 joules), (positive print).

case by dividing the measured flash duration by the ratio between the time obtained from the normalizing curve and the mean value of all the times obtained from these normalizing curves. These recordings give a mean value of 340 μsec for the flash duration, with a standard deviation of 12 μsec. It must be emphasized that this is *not* the flash duration to be considered in most experiments, since the latter normally involves the use of ultraviolet light where the light pulse is considerably shorter. As seen in Fig. 13, the time of the light pulse is strongly wavelength-dependent and increases with the wavelength. Certain irregularities are shown. Thus the time recorded at about 330 mμ is only one half of the time that could be expected. It is to be noted that this wavelength corresponds to very strong absorption lines in the spectrum, as is seen from the photographed spectrum in Fig. 14.

The spectral distribution of the light reaching the reaction vessel was obtained from graphical integration of the oscillograms. They were normalized in the same way as the flash durations. The mean value of the curves used for the normalization had an integrated area of 60.8, with a standard deviation of 4.2 (arbitrary units). Knowing the dispersion and the transmission of the monochromator, together with the spectral sensitivity of the photocell, it was possible to calculate the spectral distribution, which is shown in Fig. 8. It is given in absolute units. It can be noted that the intensity increases with decreasing wavelength, which is quite striking, as the flash duration decreases with decreasing wavelength.

Gas chromatography

The substances which had to be measured were carbon monoxide, hydrogen, various hydrocarbons and some organic substances containing oxygen. When quantum yield determinations are made by the help of Apparatus III very small amounts of the products are formed. The gas chromatograph thus had to have a detector which allowed quantitative analysis of components of the order of 10^{-9} g. A flame ionization detector was found to fulfil the requirements. The original construction comes from Harley, Nel and Pretorius [17]. The flame ionization detector used in the present investigation is essentially a copy of the one described by Thompson [18]. The column effluent is ionized in a hydrogen flame. Hydrogen serves as carrier gas and is introduced into the detector through a hypodermic needle, which also serves as the positive pole. A platinum gauze above the flame provides the negative electrode. Normal commercial hydrogen was used as carrier gas. The amplifier was built according to the construction described by Thompson. It was connected to a Speedomax 10 mV recorder. The air for the combustion was taken from a cylinder and filtered through glass wool. As seen in Fig. 15, the amplifier has a very good signal-to-noise ratio, even when used at highest sensitivity, and the base line drift is quite small. The chromatogram in the figure is a recording of products from the photolysis of acetaldehyde in Apparatus III. There is a high degree of linearity between the response of the recorder and the amount of substance added. Fig. 16 shows calibration curves obtained at the highest sensitivity.

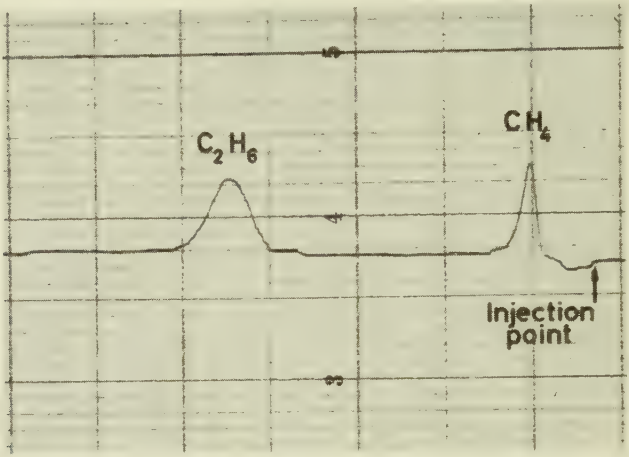

Fig. 15. Chromatogram of products from photolysis of acetaldehyde in Apparatus III using the flame ionization detector at its highest sensitivity. The amount of methane is 6.0×10^{-9} g and the amount of ethane 12.4×10^{-9} g.

Carbon monoxide and hydrogen are important constituents in the products. These products cannot be recorded by the flame ionization detector and therefore, to make their analysis possible, a highly sensitive thermal conductivity cell was constructed. The cell, which was designed to work at temperatures up to 400°C, has a volume less than 1 ml and is made of stainless steel. The detecting elements consist of tungsten wire (diam. 0.06 mm) with a resistance of 3.2 ohm fixed on a small glow plug. The possibility of using thermistors was tried, but it was determined from these experiments that, together with a good electronic amplifier, a metal wire gave a better signal-to-noise ratio. A Leeds and Northrup D.C. amplifier was used between the cell and the recorder, which was a Speedomax 10 mV. Special care was necessary to protect the detector from outside electrical disturbances and temperature variations. Even at highest amplification, the stability is extremely good and the noise level

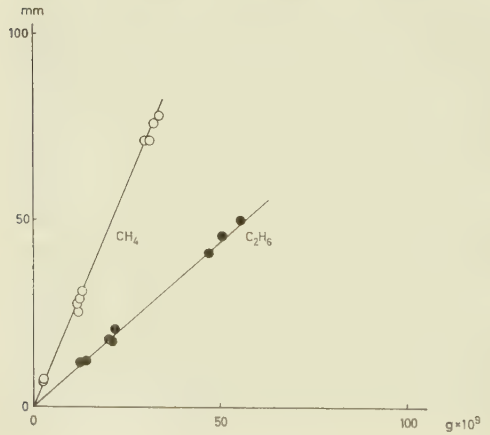

Fig. 16. Calibration curves using the flame ionization detector at its highest sensitivity. The height of the chromatogram peak is plotted as a function of amount of substance.

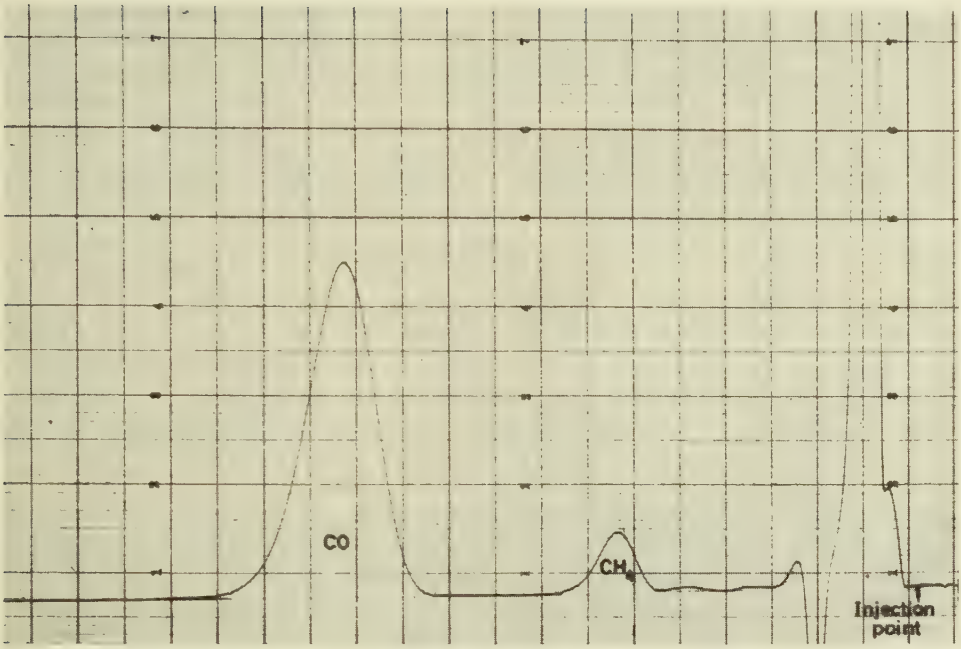

Fig. 17. Chromatogram using the thermal conductivity detector at its highest sensitivity. The amount of methane is 0.33×10^{-6} g and of carbon monoxide 3.74×10^{-6} g.

is low, as is seen in the chromatogram given in Fig. 17. The amount of methane recorded on the chromatogram is 0.33 μg and that of carbon monoxide 3.74 μg, the analysis being made with hydrogen as carrier gas. A generally satisfactory expression which gives a good quantitative measure of the sensitivity of a detector is the sensitivity parameter, S, of Dimbat, Porter and Stross [19]. Making use of the methane peak in Fig. 17, the sensitivity parameter is calculated to be $S = 34{,}000$ ml mV mg^{-1}. This value for S indicates that the cell is between ten and a hundred times more sensitive than other constructions given in the literature [20, 21]. Fig. 18 gives some calibration curves for recordings using the highest sensitivity. It is seen that there is an excellent linear relation between the area under the peak and the substance added.

The column tubes consist of stainless steel with an inner diameter of 5 mm. They are built in units of 26 and 53 cm length and can easily be combined to give a suitable column length. The column is enclosed in an electric heater. The entire gas chromatograph is described in a separate paper [22].

As mentioned above, hydrogen was the carrier gas when the flame ionization detector was used. With the thermal conductivity detector, recordings were made using either hydrogen or nitrogen as carrier gas. A great variety of stationary phases were employed. Some column fillings were prepared in the laboratory and some were bought ready-made from Perkin–Elmer Corporation. Type of detector, carrier gas, flow rate of carrier gas, column filling, column length and column temperature are specified in each table showing the analysis.

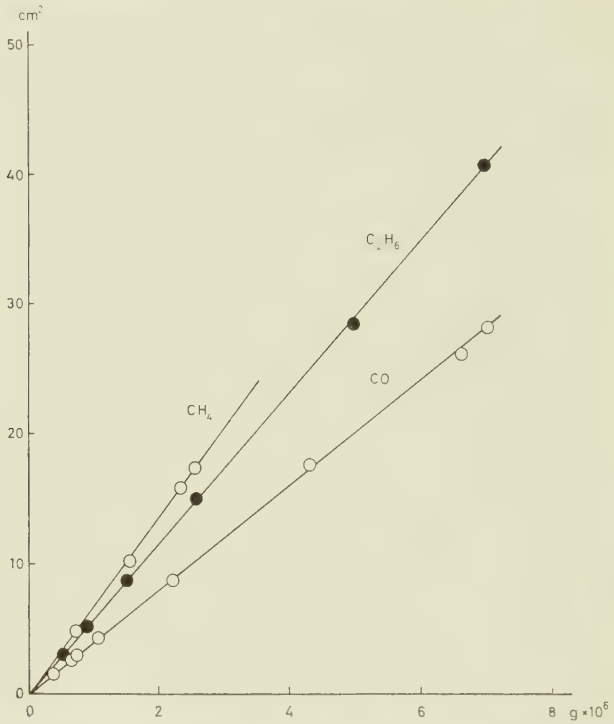

Fig. 18. Calibration curves using the thermal conductivity detector at its highest sensitivity. The area under the chromatogram peak is plotted as a function of amount of substance.

The samples are introduced in the usual way by trapping a defined volume between two valves and forcing it into the gas stream [23]. The sample from the reaction vessel is allowed to expand in a large evacuated volume and the greater part of it is then pressed into the trap by means of mercury. For a specific volume of the reaction vessel, the ratio between the total amount of sample and the amount introduced is constant. With the cells used together with Apparatus II, 87 % of the sample is introduced.

Each set of analyses with the gas chromatograph was preceded by a complete calibration for all the proposed products. This means that a considerable amount of work has been devoted to ensuring the correctness of the analytical work on all occasions. Known amounts of the substances were introduced into the reaction vessel whose contents were then transferred to the gas chromatograph in the described fashion.

Chemicals

Acetone (LKB p.a.) was fractionally distilled at atmospheric pressure and a constant-boiling fraction was redistilled under vacuum.

Acetaldehyde (Fluka AG, puriss p.a.) was mixed with a few drops of sulphuric acid and distilled twice at normal pressure. A constant-boiling fraction was used after vacuum-distillation.

Propionaldehyde, *n*-butyraldehyde and isobutyraldehyde (Eastman Kodak Company) were dried over anhydrous calcium sulphate and fractionated at atmospheric pressure. A constant-boiling fraction was further distilled under vacuum and degassed.

Helium (The Matheson Company) was taken from a storage cylinder. For the removal of possible traces of oxygen it was passed through a column with Linde Molecular Sieves 5A at low temperature.

Gas chromatographic analysis showed that all the samples were pure with respect to the products analysed for after photolysis.

Section 2. General theory

Reaction of the triplet state

Consider a molecule in the singlet ground state, S, which absorbs a quantum to give an excited singlet, S^*

$$S + h\nu \rightarrow S^*. \tag{1}$$

If this excited singlet is very short-lived, no intensity dependence of the reactions of the excited singlet will appear, even at the high intensities obtained by employing flash photolysis. The excited singlet may return to the ground state by internal conversion or fluorescence. A direct cleavage to give products and a transformation to a triplet state may also occur. Assume that a large portion of the singlet molecules is transformed to a long-lived triplet state, T

$$S^* \rightarrow T. \tag{2}$$

The rate of formation of the triplet may thus be proportional to the absorbed light intensity, I_a

$$(r_T)_f = \gamma I_a, \tag{9}$$

γ being a constant.

The following reactions seem to give a fairly complete picture of the possible reactions of the triplet

$$T + T \rightarrow 2S, \tag{3a}$$

$$T + T \rightarrow P_{3b}, \tag{3b}$$

$$T + S \rightarrow S + S, \tag{4a}$$

$$T + S \rightarrow P_{4b}(+S), \tag{4b}$$

$$T \rightarrow S, \tag{5a}$$

$$T \rightarrow P_{5b}. \tag{5b}$$

Reactions (3a), (4a) and (5a) represent the deactivation of the triplet to the ground state and reactions (3b), (4b) and (5b) the decomposition of the triplet to form products. P_{3b}, P_{4b} and P_{5b} represent the products which are formed when the triplet is split. These products may be radicals or stable molecules; part of them may also recombine to form the parent substance S. It is likely that the triplet molecules retain excess energy when they are formed, and thus collisions with a third body

will undoubtedly be of importance. It seems, however, difficult to estimate the influence of these collisions and they have not been taken into consideration.

The rate of dissipation of the triplet may then be written as[1]

$$(r_T)_d = 2\,k_{3a}[T]^2 + 2\,k_{3b}[T]^2 + k_{4a}[T][S] + k_{4b}[T][S] + k_{5a}[T] + k_{5b}[T]. \qquad \{10\}$$

If steady state conditions are applicable, the rate of formation of the triplet can be put equal to the rate of its dissipation. The concentration of the triplet will then appear from Eqs. {9} and {10} as

$$[T] = \frac{2\gamma I_a}{\{[(k_{4a}+k_{4b})[S]+k_{5a}+k_{5b}]^2 + 8(k_{3a}+k_{3b})\gamma I_a\}^{\frac{1}{2}} + (k_{4a}+k_{4b})[S]+k_{5a}+k_{5b}}. \qquad \{11\}$$

The quantum yield of decomposition of the triplet is defined as

$$\phi_T = \frac{2\,k_{3b}[T]^2 + k_{4b}[T][S] + k_{5b}[T]}{I_a}. \qquad \{12\}$$

It is possible that at the high intensities obtained with flash apparatus, the reactions which are second order with respect to triplet concentration will be of great importance.

One may isolate the following two cases:

1. Reactions (3a) and (3b) are the predominant reactions of the triplet (triplet–triplet reactions predominate)

$$\phi_T = \frac{\gamma k_{3b}}{k_{3a}+k_{3b}} + \frac{\gamma^{\frac{1}{2}} k_{4b}}{(2\,k_{3a}+2\,k_{3b})^{\frac{1}{2}}}[S] I_a^{-\frac{1}{2}} + \frac{\gamma^{\frac{1}{2}} k_{5b}}{(2\,k_{3a}+2\,k_{3b})^{\frac{1}{2}}} I_a^{-\frac{1}{2}}. \qquad \{13\}$$

2. Reactions (3a) and (3b) are negligible (triplet–triplet reactions are negligible)

$$\phi_T = \frac{\gamma k_{4b}[S]}{(k_{4a}+k_{4b})[S]+k_{5a}+k_{5b}} + \frac{\gamma k_{5b}}{(k_{4a}+k_{4b})[S]+k_{5a}+k_{5b}}. \qquad \{14\}$$

From Eqs. {13} and {14} it is obvious that ϕ_T can be expected to be intensity dependent at high light intensities and not at low light intensities. The three terms in Eq. {13} describe the contribution to ϕ_T from reactions (3b), (4b) and (5b) respectively. Similarly, the two terms in Eq. {14} describe the contribution to ϕ_T from reactions (4b) and (5b) respectively.

Radical reactions

Assume that the molecule M can dissociate in one or several ways, whereby the radicals R_1 and R_2 are formed, in some cases together with stable molecules. Some of the dissociation processes produce R_1 and R_2 radicals, whereas others produce R_1 *or* R_2 radicals. It is then possible to describe the mean of these processes as

$$M \rightarrow a\,R_1 + b\,R_2(+P_6), \qquad (6)$$

where P_6 represents stable molecules formed.

[1] In the following, k_n denotes the rate constant of reaction (n) and $[A]$ the concentration of A.

The following reactions are then likely

$$R_1 + R_1 \rightarrow P_7, \tag{7}$$

$$R_1 + R_2 \rightarrow P_8, \tag{8}$$

$$R_2 + R_2 \rightarrow P_9, \tag{9}$$

$$R_1 + M \rightarrow P_{10}, \tag{10}$$

$$R_2 + M \rightarrow P_{11}, \tag{11}$$

where P_n is the product(s) formed in reaction (n). The products $P_6 - P_{11}$ may be in part identical; parent molecules, M, may also be formed in reactions (7) to (11).

The rate of dissipation of the radical R_1 is thus

$$(r_{R_1})_d = 2k_7[R_1]^2 + k_8[R_1][R_2] + k_{10}[R_1][M], \tag{15}$$

and the rate of dissipation of the radical R_2

$$(r_{R_2})_d = k_8[R_1][R_2] + 2k_9[R_2]^2 + k_{11}[R_2][M]. \tag{16}$$

The following relation is valid[1]

$$r_6 = \frac{(r_{R_1})_f}{a} = \frac{(r_{R_2})_f}{b}, \tag{17}$$

where $(r_{R_1})_f$ and $(r_{R_2})_f$ are the rates of formation of the radicals R_1 and R_2 respectively.

In the following, steady state conditions are assumed to be applicable; the rate of formation of a radical is put equal to its rate of dissipation. If the radical–radical reactions predominate, the final terms in Eqs. {15} and {16} can be neglected and one obtains

$$\frac{[R_1]}{[R_2]} = \frac{4ak_9}{(b-a)k_8 + [(b-a)^2k_8^2 + 16abk_7k_9]^{\frac{1}{2}}} = K_{18}. \tag{18}$$

In the specific case where $a = b$, this expression will reduce to

$$\frac{[R_1]}{[R_2]} = \left(\frac{k_9}{k_7}\right)^{\frac{1}{2}}. \tag{19}$$

This means that if the reactions which are second order with respect to radical concentration predominate, the ratio between the radical concentrations will be constant. It is thus obvious that under these circumstances the quotient of the yields of products from any two second order radical reactions will be independent of the rate of formation of the radicals. The quotient of the rates of reaction (7) and (8) is given as

$$\frac{r_7}{r_8} = K_{18}\frac{k_7}{k_8}. \tag{20}$$

[1] In the following, r_n denotes the rate of reaction (n).

It is seen from Eq. {18} that if $a \geqslant b$, the following relationship is valid

$$K_{18} \geqslant \left(\frac{k_9}{k_7}\right)^{\frac{1}{2}}. \qquad \{21\}$$

Furthermore, as the final terms in Eqs. {15} and {16} are neglected the concentration of the radical R_1 is given as

$$[R_1] = \left(\frac{a r_6}{2 k_7 + \frac{k_8}{K_{18}}}\right)^{\frac{1}{2}}. \qquad \{22\}$$

Quantum yields for the formation of products

If radical–radical reactions predominate, it is possible to derive simple relations between the quantum yield for the formation of a product and the quantum yield of dissociation of M. Considering the reactions of the radical R_1 in the reactions (7) and (10), the quantum yields are defined from Eqs. {15} – {18} as

$$\phi_{P_7} = \frac{k_7 [R_1]^2}{I_a}, \qquad \{23\}$$

$$\phi_{P_{10}} = \frac{k_{10} [R_1][M]}{I_a}, \qquad \{24\}$$

where ϕ_{P_7} and $\phi_{P_{10}}$ are the quantum yields of formation of the products P_7 and P_{10} respectively. Combining these equations with Eq. {22} gives

$$\phi_{P_7} = \frac{k_7 a r_6}{\left(2 k_7 + \frac{k_8}{K_{18}}\right) I_a} = \frac{a k_7}{\left(2 k_7 + \frac{k_8}{K_{18}}\right)} \phi_M, \qquad \{25\}$$

$$\phi_{P_{10}} = \frac{k_{10} a^{\frac{1}{2}} r_6^{\frac{1}{2}} [M]}{\left(2 k_7 + \frac{k_8}{K_{18}}\right)^{\frac{1}{2}} I_a} = \frac{a^{\frac{1}{2}} k_{10}}{\left(2 k_7 + \frac{k_8}{K_{18}}\right)^{\frac{1}{2}}} [M] I_a^{-\frac{1}{2}} \phi_M^{\frac{1}{2}}, \qquad \{26\}$$

where ϕ_M is the quantum yield of dissociation of M. It should be noted that if the values of a and b remain constant, there is a direct proportionality between the quantum yield of formation of the product P_7 and the quantum yield of dissociation of M. This proportionality between the quantum yield of a product and the quantum yield of dissociation of M extends to all radical–radical reactions.

The quantum yield for a direct dissociation from the excited singlet will be independent of the absorbed intensity or the pressure of the substance. On the other hand, the quantum yield of dissociation from the triplet can be expected to show a dependence on these variables. Reaction (6) represents the net result of all dissociation processes of the triplet molecule. It is seen that a change in the relative impor-

tance of the different dissociation processes will then affect the values of a and b. The function describing the quantum yield of formation of a product as a function of the quantum yield of reaction (6) will thus be complex, compare Eqs. {18}, {25} and {26}.

Dissociation of the triplet is the only radical-forming process.—In the specific case, when no radicals are formed from a dissociation of the excited singlet and the only radical-forming reaction is the decomposition of the triplet, some simple relations can be deduced between the quantum yield for the formation of a product and the absorbed intensity and the concentration of the photolyzed substance. A scheme of the reactions of the triplet was given on page 21. It seems convenient to consider particular cases, in which different assumptions are made about the relative importance of reactions (3a)–(5b), and in these cases evaluate the quantum yield of formation of a product as a function of the absorbed intensity and the concentration of the sample. It is expected that when flash photolysis is employed, the radical–radical reactions will predominate and Eq. {25} will be valid. The quantum yield for the formation of the product P_7 can then be described in the following way:

1. Deactivation to the ground state in triplet–triplet collisions is the predominant reaction of the triplet.

Reaction (3b) is the predominant dissociation process,

$$\phi_{P_7} = \frac{a\,k_7}{2\,k_7 + \dfrac{k_8}{K_{18}}} \cdot \frac{\gamma\,k_{3b}}{k_{3a} + k_{3b}}. \qquad \{27\}$$

Reaction (4b) is the predominant dissociation process,

$$\phi_{P_7} = \frac{a\,k_7}{2\,k_7 + \dfrac{k_8}{K_{18}}} \cdot \frac{\gamma^{\frac{1}{2}}\,k_{4b}}{(2\,k_{3a} + 2\,k_{3b})^{\frac{1}{2}}}\,[S]\,I_a^{-\frac{1}{2}}. \qquad \{28\}$$

Reaction (5b) is the predominant dissociation process,

$$\phi_{P_7} = \frac{a\,k_7}{2\,k_7 + \dfrac{k_8}{K_{18}}} \cdot \frac{\gamma^{\frac{1}{2}}\,k_{5b}}{(2\,k_{3a} + 2\,k_{3b})^{\frac{1}{2}}}\,I_a^{-\frac{1}{2}}. \qquad \{29\}$$

2. Reactions which are second order with respect to triplet concentration are negligible.

Reaction (4b) is the predominant dissociation process,

$$\phi_{P_7} = \frac{a\,k_7}{2\,k_7 + \dfrac{k_8}{K_{18}}} \cdot \frac{\gamma\,k_{4b}\,[S]}{(k_{4a} + k_{4b})\,[S] + k_{5a} + k_{5b}}. \qquad \{30\}$$

Reaction (5 b) is the predominant dissociation process,

$$\phi_{P_7} = \frac{a\,k_7}{2\,k_7 + \dfrac{k_8}{K_{18}}} \cdot \frac{\gamma\,k_{5b}}{(k_{4a} + k_{4b})\,[S] + k_{5a} + k_{5b}}. \qquad \{31\}$$

Estimation of radical concentration

A value for r_6 can be estimated from the amount of R_1 radicals consumed in the formation of products per unit volume, ψ_{R_1}, and the time of exposure, τ, thus

$$r_6 \approx \frac{\psi_{R_1}}{a\,\tau}. \qquad \{32\}$$

Inserting Eq. {32} in Eq. {22} gives an estimate of the concentration of the radical R_1

$$[R_1] \approx \left(\frac{\psi_{R_1}}{\left(2\,k_7 + \dfrac{k_8}{K_{18}}\right)\tau} \right)^{\frac{1}{2}}. \qquad \{33\}$$

For the systems investigated it is not possible to evaluate the value of k_8/K_{18}. As however P_7 in all these cases is a major product of the radical R_1, the two final terms in Eq. {15} can be neglected in order to obtain an estimation of the concentration of the radical R_1. One thus obtains from Eqs. {15}, {17} and {32}

$$[R_1] \approx \left(\frac{\psi_{R_1}}{2\,k_7\,\tau} \right)^{\frac{1}{2}}. \qquad \{34\}$$

Ratio between first and second order reaction rates

The ratio between the rates of reactions (10) and (7) is

$$\frac{r_{10}}{r_7} = \frac{k_{10}\,[\mathrm{M}]}{k_7\,[R_1]}. \qquad \{35\}$$

When Eq. {22} holds, one gets

$$\frac{r_{10}}{r_7} = \frac{k_{10}}{k_7} \left(2\,k_7 + \frac{k_8}{K_{18}}\right)^{\frac{1}{2}} \frac{[M]}{a^{\frac{1}{2}}\,r_6^{\frac{1}{2}}}. \qquad \{36\}$$

From Eqs. {34} and {35} it is obvious that

$$\frac{r_{10}}{r_7} \approx 2^{\frac{1}{2}} \frac{k_{10}}{k_7^{\frac{1}{2}}} \left(\frac{\tau}{\psi_{R_1}}\right)^{\frac{1}{2}} [M]. \qquad \{37\}$$

The ratio between the rates of reactions (10) and (7) can thus be estimated by Eq. {37} if reaction (7) is a major reaction of the radical R_1.

Section 3. Results and discussion

General presentation and consideration

Apparatus II

The results from the photolysis carried out using Apparatus II are given in Tables 2–6 and Tables 8–24. All major products have been recorded. In each table, the data are arranged in order of increasing pressures of the photolyzed substance. Some tables are divided into two sections indicating that each section has been preceded by a complete calibration for the recorded products. In many cases it has been possible to determine several components from the same chromatogram. This is quite important, as a more accurate value for the ratio between two products is obtained in this way. In the case of *n*-butyraldehyde, seven components were determined simultaneously from a chromatogram where tetraethylene glycol dimethyl ether was used as stationary phase (Table 21).

Effect of temperature.—The temperature rise in the reaction mixture which was associated with the quantum yield determinations in Apparatus III is discussed below. In the case of irradiation with Apparatus II, this quantity cannot easily be calculated, as the absorbed light dose is not known. The quantum yields determined with Apparatus III are not applicable in this case, as the spectral distribution of the light absorbed is drastically changed. In fact, very much higher quantum yields can be expected for irradiations with Apparatus II, as lower wavelengths are involved. The temperature change when the substance is irradiated in the absence of inert gas may amount to several hundred degrees.

In order to increase the heat capacity of the system and thus reduce the reaction temperature, helium was added to the sample in some experiments. This addition of helium did not affect the product yields to any great extent. Only in the case of acetone were significant changes observed in the amounts of the formed products. In all other cases, the addition of helium was found to cause only minor changes which lie within the limits of experimental error. Tables 2–5 show the results from acetone photolysis obtained both in the absence and in the presence of helium. When helium was used, it was added in an amount sufficient to make the pressure of the reaction mixture equal to atmospheric before photolysis. The values in Table 6 and Tables 8–24 are data obtained from photolysis of the substance alone.

Due to the interference of helium in analyses for hydrogen, no measurements of the formation of hydrogen have been made in those cases where helium was added to the reaction mixture.

Apparatus III

The quantum yield determinations using Apparatus III are summarized in Table 7 and Tables 25–28. For the photolysis of acetone, the quantum yield of ethane formation was determined. In the chromatograms, small methane peaks appeared which showed that methane is formed in a quantity equivalent to about 10 % of that of ethane. The quantum yields of the formation of methane and ethane were calculated for the photolysis of acetaldehyde, and for the photolysis of propionaldehyde the quantum yield of ethane. Quantum yields of propane production were

determined for *n*-butyraldehyde and isobutyraldehyde. For *n*-butyraldehyde the quantum yield of ethylene formation was also determined.

For the photolysis of acetone, acetaldehyde and propionaldehyde, the quantum yields are plotted as a function of the pressure of the parent substance in Figs. 21, 25 and 26. It is seen that the quantum yields increase strongly with decreasing pressures.

The ratio between the quantum yield of methane and the quantum yield of ethane for acetaldehyde photolysis increases markedly at higher acetaldehyde pressures.

Effect of temperature.—It is calculated that about 0.5 % of the molecules absorb a quantum. Assuming adiabatic conditions, a value for the temperature change resulting from the absorbed light can be estimated. The energy dissipation from fluorescence and phosphorescence is neglected as is the energy of reaction, which is quite small. Using an average value of 280 mμ for the wavelength and 18 cal degree^{-1} mole^{-1} for the molar heat capacity at constant volume, the temperature change is calculated to be about 30°C during the photolysis of acetone. A similar calculation for acetaldehyde yields a temperature rise of about 45°C. The heat capacities of propionaldehyde, *n*-butyraldehyde and isobutyraldehyde are higher than that of acetaldehyde, whereas the absorbed light dose is about the same, and thus the temperature rise will be smaller. It is clear, then, that the temperature change is by no means insignificant.

To check whether a change in quantum yield could be expected at lower reaction temperatures, the following experiments were undertaken. Acetone, acetaldehyde and propionaldehyde were photolyzed at a pressure of about 150 mm Hg. Helium was added to make the pressure of the total reaction mixture equal to atmospheric before photolysis, the heat capacity of the system thus being increased. No effects on the quantum yields as a result of the presence of the helium were found within the limits of experimental error. It seems quite unlikely that the addition of helium, besides its effect on the temperature, also influences the quantum yield in another way such that the two effects cancel each other out.

Steady state

The theoretical derivations were carried out on the assumption that steady state conditions are applicable. A simple calculation will provide information about the time that is needed to reach a steady state.

It seems useful to compare the amount of a radical in a steady state concentration with the amount of products formed as a result of reactions of that radical. An upper limit for the radical concentration is defined by Eq. {34}. Identifying R_1 with the methyl radical, it is possible to make an estimation of its concentration on the basis of the calculated value of its rate constant of recombination. This rate constant is given by Shepp to be 2.2×10^{13} cm^3 mole^{-1} sec^{-1} [24].

Consider the photolysis of acetone at 100 mm Hg pressure. In apparatus II a yield of ethane of about 4×10^{-7} mole was obtained and an estimate for ψ_{R_1} in Eq. {34} can thus be given as two times the ethane yield divided by the volume of the reaction vessel. With a flash period, τ, of 1.0×10^{-5} sec the methyl radical concentration, calculated from Eq. {34}, is 2×10^{-8} mole cm^{-3}. When acetone was photolyzed at a pressure of 100 mm Hg in Apparatus III, the ethane yield was found to be about 4×10^{-10} mole. Taking 3×10^{-4} sec as the flash period (Fig. 13),

the methyl radical concentration is calculated to be 2×10^{-10} mole cm^{-3} from Eq. {34}.

From the above calculations, then, it seems possible that the time needed to reach a steady state is of the same magnitude as the flash duration.

Acetone

The products recorded in the photolysis of acetone in Apparatus II are carbon monoxide, methane, ethane, biacetyl, methyl ethyl ketone, acetaldehyde and hydrogen. Product yields are plotted as a function of acetone pressure in Figs. 19 and 20. All curves, with the possible exception of that for methane, become progressively less steep at increased pressures. These effects are particularly pronounced for biacetyl and methyl ethyl ketone. It is found that the carbon monoxide and ethane yields are very little affected by the addition of helium, while there is no effect at all on the yield of methyl ethyl ketone. On the other hand, the methane yield increases markedly on the addition of helium, whereas the yield of biacetyl and acetaldehyde decreases.

Mass balance

At an acetone pressure of 80 mm Hg mass balance calculations on the products give the following mole ratios:

$$\frac{H}{C} = 2.10 \quad \frac{O}{C} = 0.31 \quad \text{in the absence of helium,}$$

$$\frac{H}{C} = 2.15 \quad \frac{O}{C} = 0.30 \quad \text{in the presence of helium.}$$

The product yields at 80 mm Hg are taken from the graphs in Figs. 19 and 20 and from Table 5. The yield of hydrogen, in the absence of helium, is taken as 1×10^{-8} mole from Table 6. No analysis of the yield of hydrogen was made when helium was present during photolysis, and therefore no value for hydrogen has been introduced into the mole ratios in this case.

The above mole ratios should be compared to the following mole ratios for acetone

$$\frac{H}{C} = 2.00 \quad \frac{O}{C} = 0.33.$$

The apparent discrepancy between the experimentally determined mole ratios for the products and those for acetone is probably largely due to the existence of other products, e.g. ketene, diacetonyl and acetylacetone, which have not been analyzed for. The compositions of these substances are such that, were they taken into account, the mole ratios for the products would probably be brought closer to those for acetone.

Primary dissociation processes

A primary dissociation process has been accepted to be the splitting of the acetone molecule into a methyl radical and an acetyl radical [3, 4],

$$CH_3COCH_3 + h\nu \rightarrow CH_3 + CH_3CO. \quad (P12)$$

The direct dissociation of the acetone molecule into two methyl radicals and carbon monoxide has also been proposed to contribute to the primary process,

$$CH_3COCH_3 + h\nu \rightarrow 2CH_3 + CO. \quad (P13)$$

It has been pointed out that the contribution of reaction (P13) can be represented in another manner. According to this representation, part of the acetyl radicals produced in reaction (P12) retain sufficient energy to undergo a spontaneous decomposition into methyl radicals and carbon monoxide,

$$CH_3CO^* \rightarrow CH_3 + CO. \quad (14)$$

Decrease in the wavelength of the light will cause an increase in the portion of the acetyl radicals which have been given enough energy in the primary dissociation to allow them to undergo spontaneous decomposition.

To account for the considerable amount of hydrogen found when light of shorter wavelengths is used, another primary dissociation process (P15) has also been proposed,

$$CH_3COCH_3 + h\nu \rightarrow CH_3COCH_2 + H. \quad (P15)$$

This reaction involves the dissociation of the acetone molecule into an acetonyl radical and a hydrogen atom and is assumed to occur in the banded region of the acetone spectrum, below 200 mμ. The results of the present investigation appear to be in agreement with this assumption. Thus, hydrogen was found as a minor component amongst the products, while the light emitted from the flash lamp contains appreciable quantities of ultraviolet light of fairly short wavelength.

Simplified reaction scheme for the radicals

The primary dissociation process (P15) must be considered, but clearly constitutes only a minor part of the total dissociation. If we then neglect reaction (P15), the system will, after photolysis, contain the radicals methyl and acetyl. The postulated reactions which will occur between these radicals are

$$CH_3 + CH_3 \rightarrow C_2H_6, \quad (16)$$

$$CH_3CO + CH_3CO \rightarrow (CH_3CO)_2, \quad (17a)$$

$$CH_3CO + CH_3CO \rightarrow CH_3CHO + CH_2CO, \quad (17b)$$

$$CH_3 + CH_3CO \rightarrow CH_3COCH_3, \quad (18a)$$

$$CH_3 + CH_3CO \rightarrow CH_4 + CH_2CO. \quad (18b)$$

Acetyl radicals which have come into thermal equilibrium are known to undergo a rapid decomposition

$$CH_3CO \rightarrow CH_3 + CO. \quad (19)$$

Calvert has recently discussed the activation energy of reaction (19) and has calculated the rate constant to be $k = 1.6 \times 10^9 \exp(-12000 \pm 2000/\boldsymbol{R}T)\text{sec}^{-1}$ [25]. It seems, however, that there exists considerable uncertainty about the nature of this reaction.

Methyl radicals are known to abstract hydrogen atoms in a reaction with acetone molecules

$$CH_3 + CH_3COCH_3 \rightarrow CH_4 + CH_3COCH_2. \qquad (20)$$

In order to get an estimate of the occurrence of this reaction, it seems useful to compare the rate of reactions (20) and (16). The ratio of these two rates is

$$\frac{r_{20}}{r_{16}} = \frac{k_{20}[CH_3COCH_3]}{k_{16}[CH_3]}. \qquad \{38\}$$

If the reactions which are second order with respect to radical concentration predominate, it is useful to identify CH_3COCH_3 with M, and CH_3 with R_1, page 22. That the second order reactions predominate seems to be the case, as in all present experiments the ethane yields are much higher than the methane yields. Using Eq. {37} one then obtains

$$\frac{r_{20}}{r_{16}} \approx 2^{\frac{1}{2}} \frac{k_{20}}{k_{16}^{\frac{1}{2}}} \left(\frac{\tau}{\psi_{CH_3}}\right)^{\frac{1}{2}} [CH_3COCH_3]. \qquad \{39\}$$

The ratio $k_{20}\, k_{16}^{-\frac{1}{2}}$ has been carefully estimated by Ausloos and Steacie from a photolysis study of azomethane-acetone mixtures [26]. They obtained values rising from 1.35×10^{-14} to 69.0×10^{-14} $\text{cm}^{\frac{3}{2}}$ $\text{molecule}^{-\frac{1}{2}}$ $\text{sec}^{-\frac{1}{2}}$ as the temperature was increased from 26 to 140°C.

For the photolysis of acetone in Apparatus III, the temperature rise was calculated to be about 30°C, page 28. If thus 50°C is taken as the reaction temperature, the value of $k_{20}\, k_{16}^{-\frac{1}{2}}$ is obtained as 4×10^{-14} $\text{cm}^{\frac{3}{2}}$ $\text{molecule}^{-\frac{1}{2}}$ $\text{sec}^{-\frac{1}{2}}$ from reference [26]. Twice the measured yield of ethane divided by the cell volume, gives an estimate of the amount of methyl radicals consumed per unit volume, ψ_{CH_3}. Taking 3×10^{-4} sec as the flash duration (Fig. 13), the value of r_{20}/r_{16} is given as 0.0003 at maximum acetone pressure, from Eq. {39}. It is thus improbable that the methane obtained with Apparatus III arises by reaction (20).

The flash duration in Apparatus II is about thirty times shorter than in Apparatus III, while the reaction temperature is not known. The ratio of the yields of methane and ethane was found to increase with increasing acetone pressures, which is to be expected if methane is formed in a first order reaction, compare Eq. {36}. It was, however, found that the yield of methane strongly increased with the addition of helium, which lowers the reaction temperature, whereas the value of $k_{20}/k_{16}^{\frac{1}{2}}$ is known to decrease at decreased reaction temperatures. Another reaction producing methane must therefore be sought for in this case.

It has clearly been demonstrated that reaction (16) occurs via an excited complex which is stabilized by collision with a third body [27, 28],

$$CH_3 + CH_3 \rightarrow C_2H_6^*, \qquad (16')$$

$$C_2H_6^* + B \rightarrow C_2H_6 + B, \qquad (16'')$$

Table 2. Photolysis of acetone in Apparatus II. Determination of the yields of methane (CH_4), and carbon monoxide (CO).

Detector: Thermal conductivity.
Carrier gas: Hydrogen (H_2).
Flow rate of carrier gas. 20 cm^3 min^{-1}.
Stationary phase: Linde Molecular Sieves 5A (30–52 mesh).
Column length: 106 cm.
Column temperature: 45°C.

Medium	Pressure of acetone before photolysis mm Hg	Yield of methane (Ψ_{CH_4}) mole × 10^8	Yield of carbon monoxide (Ψ_{CO}) mole × 10^8	$\frac{\Psi_{CH_4}}{\Psi_{CO}}$
Helium not present	25.5	0.8	13.9	0.06
	28.1	0.6	12.5	0.05
	46.6	1.2	17.9	0.07
	48.4	1.2	18.9	0.06
	54.4	failure	18.9	—
	102.4	1.9	33.6	0.06
	107.1	2.4	40.7	0.06
	112.3	2.4	35.7	0.07
	163.6	4.4	53.9	0.08
	173.4	4.0	53.2	0.08
	173.8	4.3	51.1	0.08
Helium added to a total pressure of one atmosphere	27.9	2.3	8.8	0.26
	28.4	1.8	10.6	0.17
	38.9	1.4	9.3	0.15
	53.0	3.0	17.0	0.18
	57.5	3.0	16.5	0.18
	75.0	failure	24.4	—
	83.0	3.4	20.3	0.17
	86.8	3.1	23.7	0.13
	103.2	4.0	28.2	0.14
	153.7	5.5	42.1	0.13
	172.0	7.1	48.2	0.15
	174.5	7.8	44.3	0.18

B representing the third body. A value for the rate constant k_{16} has been calculated by Shepp from photolysis studies with intermittent light [24]. It seems to have been established that reaction (16) proceeds with a collision efficiency not far from unity at the pressures used in the present investigation.

Biacetyl appears as one of the products, doubtlessly due to a recombination of two acetyl radicals, reaction (17a). The collision of two acetyl radicals may also result in a disproportionation reaction (17b) to form acetaldehyde and ketene [26, 29]. The question of homogeneous versus wall recombination of the acetyl radicals in reaction (17a) has lent an uncertainty to the interpretation of the low intensity data. The various findings have been summarized by Steacie [3]. Most of the conclusions are based on the results of more indirect data. However, direct evidence for the formation of biacetyl on the wall is provided by the experiments of Glazebrook and Pearson, who found that no biacetyl appeared when the walls of the vessels were coated with tellurium [30]. The disagreements in the results of the various

Table 3. Photolysis of acetone in Apparatus II. Determination of the yield of ethane (C_2H_6).

Detector: Thermal conductivity.
Carrier gas: Hydrogen (H_2).
Flow rate of carrier gas: 30 cm^3 min^{-1}.
Stationary phase: Linde Molecular Sieves 5A (30–52 mesh).
Column length: 106 cm.
Column temperature: 180°C.

Medium	Pressure of acetone before photolysis mm Hg	Yield of ethane ($\Psi_{C_2H_6}$) mole × 10^8
Helium not present	22.5	14.7
	23.5	16.0
	49.0	29.3
	50.1	27.7
	92.0	43.7
	95.9	36.0
	99.0	43.3
	160.3	54.0
	163.1	56.3
Helium added to a total pressure of one atmosphere	28.0	11.7
	28.3	12.0
	60.8	22.3
	61.0	19.3
	100.6	37.0
	103.5	36.7
	161.4	47.7
	171.4	46.7

workers are explained if reaction (17a) proceeds heterogeneously at lower intensities and homogeneously at higher intensities [3]. The intensities used in this earlier work were in the range of 10^{15} quanta sec^{-1} $litre^{-1}$. It can therefore be concluded that reaction (17a) will be entirely homogeneous at our intensities, which are about a milliard times higher. The yields of both biacetyl and acetaldehyde were found to decrease when helium was added to the reaction mixture. This implies that in the presence of helium, either the consumption of acetyl radicals in other reactions than (17a) and (17b) is increased, or else less acetyl radicals are formed. The possibility of an increased decomposition of the acetyl radical also exists.

The quantum yield determination in Apparatus III showed a very low value for the formation of ethane. This suggests a high efficiency for reaction (18a), which represents the recombination of the acetyl and methyl radicals to form acetone. Naldrett concluded that this reaction is responsible for the low over-all quantum efficiency of decomposition at low light intensities (of the order of 10^{15} quanta sec^{-1} $litre^{-1}$) [31]. It has been proposed that small quantities of methane and ketene arise in a disproportionation reaction between a methyl and an acetyl radical (18b) [26, 32]. The observed pressure dependence of the methane yield shows that reaction (18b) can only make a small contribution to the observed methane yields, unless three body collisions are involved.

In their review, Noyes, Porter and Jolley estimated the fraction of the acetyl

Table 4. Photolysis of acetone in Apparatus II. Determination of the yields of biacetyl ($(CH_3CO)_2$), and methyl ethyl ketone ($CH_3COC_2H_5$).

Detector: Thermal conductivity.
Carrier gas: Hydrogen (H_2).
Flow rate of carrier gas: 22 cm^3 min^{-1}.
Stationary phase: Polyethylene glycol 400 (Griffin and George) on celite (30–60 mesh).
Column length: 106 cm.
Column temperature: 45°C.

Medium	Pressure of acetone before photolysis mm Hg	Yield of biacetyl ($\Psi_{(CH_3CO)_2}$) mole × 10^8	Yield of methyl ethyl ketone ($\Psi_{CH_3COC_2H_5}$) mole × 10^8	$\frac{\Psi_{(CH_3CO)_2}}{\Psi_{CH_3COC_2H_5}}$
Helium not present	27.3	1.80	0.15	12
	32.2	1.86	0.25	7.4
	54.3	3.63	0.38	9.6
	61.2	3.97	0.64	6.2
	94.1	4.57	0.76	6.0
	102.5	4.94	0.89	5.6
	106.0	4.85	0.79	6.1
	159.3	5.21	0.75	6.9
	166.5	5.12	0.81	6.3
Helium added to a total pressure of one atmosphere	30.0	1.28	0.14	9.1
	38.9	1.51	0.33	4.6
	58.3	1.74	0.39	4.5
	65.2	1.86	0.44	4.2
	100.0	2.56	0.78	3.3
	103.8	2.67	0.74	3.6
	149.8	3.49	0.81	4.3
	157.5	3.14	0.69	4.6

radicals, formed in the primary dissociation process (P12), which will undergo spontaneous decomposition (reaction (14)) [4]. Representing the entire dissociation process by (P12), they estimated the fractions to be 0.07 at 313 mμ and 0.22 at 253.7 mμ. The light emitted from the flash lamp of Apparatus II has a continuous spectrum, which has superimposed lines and is rather constant throughout the quartz ultraviolet region, the low wavelength limit being set by the absorption of the quartz. It is thus to be expected that irradiation with Apparatus II should give high yields of carbon monoxide. The ratio between the production of carbon monoxide and the production of biacetyl, which is observed as the result of the photolysis in Apparatus II, is, however, much too high to be due to the nature of the flash lamp spectrum. There seem to be two possible explanations for this. Either the thermal decomposition of the acetyl radical is greater in the present investigation, or the dissociation process which produces acetyl radicals is diminished.

Reactions of the electronically-excited states

Acetone vapour fluoresces and phosphoresces when exposed to ultraviolet light. The quantum yields for these processes are low [10, 33].

The primary process in the photolysis of ketones was discussed in detail by Noyes, Porter and Jolley [4]. They visualized that the absorption of a quantum produces

Table 5. Photolysis of acetone in Apparatus II. Determination of the yield of acetaldehyde (CH_3CHO).

Detector: Flame ionization.
Carrier gas: Hydrogen (H_2).
Flow rate of carrier gas: 20 cm^3 min^{-1}.
Stationary phase: Perkin-Elmer F (tetra ethylene glycol dimethyl ether).
Column length: 52 cm.
Column temperature: 50°C.

Medium	Pressure of acetone before photolysis mm Hg		Yield of acetaldehyde (Ψ_{CH_3CHO}) mole × 10^8
No helium present	80.1		1.20
	80.1		1.36
	80.3		1.39
	80.5		1.59
		Mean value	1.39
Helium added to a total pressure of one atmosphere	80.0		0.80
	80.0		0.76
	80.1		0.69
	80.4		0.85
		Mean value	0.78

Table 6. Photolysis of acetone in Apparatus II. Determination of the yield of hydrogen (H_2).

Detector: Thermal conductivity.
Carrier gas: Nitrogen (N_2).
Flow rate of carrier gas: 10 cm^3 min^{-1}.
Stationary phase: Linde Molecular Sieves 5A (30–52 mesh).
Column length: 106 cm.
Column temperature: 20°C.

	Pressure of acetone before photolysis mm Hg	Yield of hydrogen (Ψ_{H_2}) mole × 10^8
No helium present	43.0	0.56
	53.0	0.45
	61.5	0.66
	102.0	1.16
	102.0	1.36
	107.0	1.53
	119.2	1.42
	154.0	0.88
	160.3	1.11
	169.0	1.07

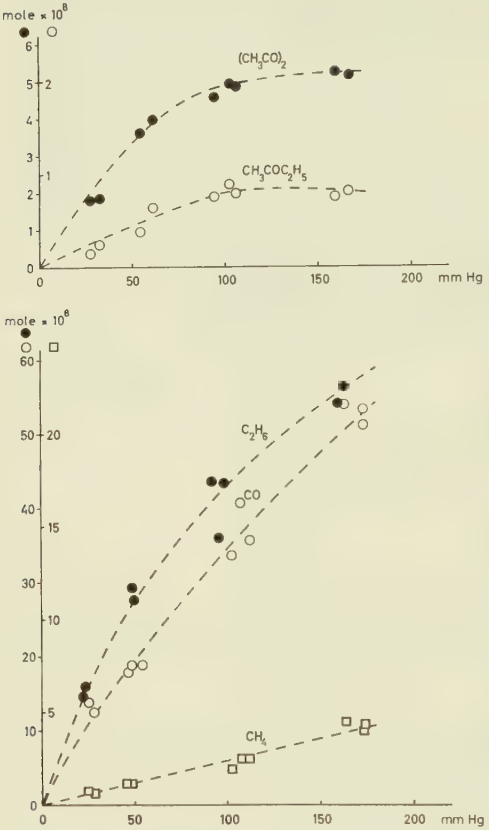

Fig. 19. Photolysis of acetone in Apparatus II. Product yields are plotted as a function of the pressure of acetone before photolysis. No helium was present.

an upper singlet state, whose vibrational energy is determined by the wavelength of the absorbed light. In the upper singlet state, some molecules dissociate, sometimes via a triplet state, while others lose vibrational energy by collision. The molecules fluoresce and phosphoresce from low vibrational levels of the singlet and the triplet state respectively. An activation energy is needed for the molecules to dissociate in the triplet state which should explain the rise in primary quantum yield and the fall in phosphorescence quantum yield with increasing temperature.

Using absorbed intensities of the order of 10^{15} quanta sec^{-1} $litre^{-1}$, Heicklen and Noyes photolyzed acetone to very low conversions and studied the fluorescence and the photolysis of acetone–biacetyl mixtures [10]. The light emission from acetone was more extensively studied by Heicklen [33]. These workers presented the following mechanism.

The absorption of a quantum produces an excited singlet state in an upper vibrational level,

$$K + h\nu = K_n^1. \tag{21}$$

This excited singlet may

(22) collide and lose vibrational energy to reach a low vibrational level in the upper singlet state,

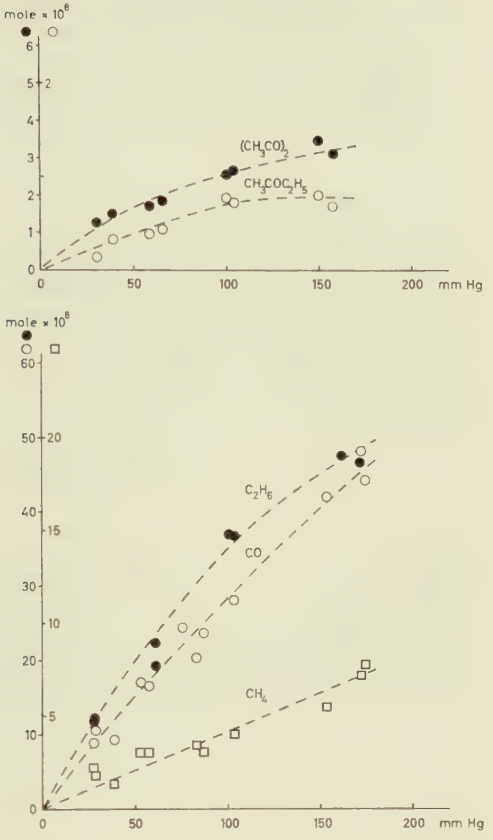

Fig. 20. Photolysis of acetone in Apparatus II. Product yields are plotted as a function of the pressure of acetone before photolysis. Helium was added in sufficient amount to give a total pressure of one atmosphere before photolysis.

(23) dissociate, D representing the dissociation products without specifying their nature,

(24) be converted to a triplet state in an upper vibrational level, possibly as the result of a collision with an acetone molecule.

$$K_n^1 + K \rightarrow K_o^1 + K, \tag{22}$$

$$K_n^1 \rightarrow D, \tag{23}$$

$$K_n^1 (+K) \rightarrow K_m^3 (+K). \tag{24}$$

From the lower vibrational levels in the singlet state, the molecule will either

(25) fluoresce and give a molecule in the ground state, or

(26) collide with an acetone molecule and give a molecule in a low vibrational level of the triplet state.

$$K_o^1 \rightarrow K + h\nu_1, \tag{25}$$

$$K_o^1 + K \rightarrow K_o^3 + K. \tag{26}$$

The triplet in the higher vibrational level may
(27) collide, and lose vibrational energy to reach a low vibrational level of the triplet state, or
(28) dissociate, D representing the dissociation products without specifying their nature.

$$K_m^3 + K \rightarrow K_o^3 + K, \tag{27}$$

$$K_m^3 \rightarrow D. \tag{28}$$

The triplet in the lower vibrational level will
(29) return to the ground state by deactivation,
(30) return to the ground state by internal conversion,
(31) return to the ground state through phosphorescence,
(32) dissociate, possibly as the result of a collision, D representing the dissociation products without specifying their nature.

$$K_o^3 + K \rightarrow K + K, \tag{29}$$

$$K_o^3 \rightarrow K, \tag{30}$$

$$K_o^3 \rightarrow K + h\nu_2, \tag{31}$$

$$K_o^3 (+K) \rightarrow D(+K). \tag{32}$$

It is suggested that
(33) the dissociation from the excited singlet state produces a carbon monoxide molecule and two methyl radicals, whereas
(34) the dissociation from the triplet state produces acetyl and methyl radicals.

$$K^1 \rightarrow 2CH_3 + CO, \tag{33}$$

$$K^3 \rightarrow CH_3CO + CH_3. \tag{34}$$

Heicklen and Noyes showed that the triplet state could be deactivated by traces of biacetyl. In the presence of this substance, the phosphorescence of acetone is diminished and biacetyl phosphorescence appears, followed by a decreased photochemical decomposition. As biacetyl is a product of the photochemical decomposition, the primary quantum yield will decrease with increased decomposition of the sample. Kaskan and Duncan observed that the lifetime of the phosphorescence of acetone was dependent on the incident intensity [34]. They explained this phenomenon on the basis of a quenching of the triplet molecule by products of the photochemical decomposition, and calculated the lifetime of the acetone triplet to be 2×10^{-4} sec. On the basis of this figure, Heicklen and Noyes estimated that a deactivation occurred every 10 to 100 collisions between the acetone triplet and the biacetyl molecule.

Using low intensities (of the order of 10^{15} quanta sec^{-1} $litre^{-1}$), the quantum yield of decomposition has been reported to lie between 0.1 and 1 [31, 35]. Roebber, Rollefson and Pimentel photolyzed acetone with a small flash photolysis apparatus which gave a maximum absorbed intensity of 4×10^{21} quanta sec^{-1} $litre^{-1}$ at an acetone pressure of 200 mm Hg [7]. The quantum yields obtained were of the same order as those obtained at lower intensities. In the present investigation, the intensities used for the determination of the quantum yields are about thirty times higher than

those used by Roebber, Rollefson and Pimentel. If the lifetime estimated for the excited molecule is correct, collisions between such molecules will be frequent enough to be of great importance in the present work. Also, reactions between excited molecules and radicals must be considered at these increased intensities.

Roebber, Rollefson and Pimentel found yields of ethane, carbon monoxide and biacetyl in proportions that could be predicted from the low intensity data. At 50 mm Hg pressure, the quantum yields of carbon monoxide and biacetyl were reported to be 0.1 and 0.2 respectively. Using a constant incident light dose, the ratio between the quantum yields of carbon monoxide and biacetyl was found to increase strongly with increasing acetone pressure. The quantum yield of carbon monoxide rose markedly with pressure. Oster and Marcus, using a constant incident flash of light, reported that the carbon monoxide yield became directly proportional to the acetone pressure if short wavelengths were removed by a cellophane filter [8]. For irradiation with the entire spectrum the curves of yield of carbon monoxide as a function of acetone pressure became progressively less steep at increasing pressures. Roebber, Rollefson and Pimentel do not give the exact procedure for the calculations of the absorbed light doses, which are needed for the determination of the quantum yields. It seems that the reported increase in carbon monoxide quantum yield with pressure should be questioned.

In the present investigation, it was shown that the curves of yields of carbon monoxide as a function of acetone pressure became progressively less steep at increasing pressures. This observation can be explained in view of the fact that acetone has two absorption regions in the ultraviolet, one at short wavelength with high extinction coefficient and the other at longer wavelength with low extinction coefficient. Consider absorption at two isolated wavelengths λ_1 and λ_2. From Eq. {4} the absorbed intensities at the two wavelengths are respectively

$$(I_a)_{\lambda_1} = (I_0)_{\lambda_1}(1 - 10^{-\alpha_{\lambda_1} pl}), \qquad \{40\}$$

$$(I_a)_{\lambda_2} = (I_0)_{\lambda_2}(1 - 10^{-\alpha_{\lambda_2} pl}). \qquad \{41\}$$

If $\alpha_{\lambda_1} \gg \alpha_{\lambda_2}$, $(I_a)_{\lambda_1}$ will soon reach the limiting value $(I_0)_{\lambda_1}$ at higher acetone pressures, whereas $(I_a)_{\lambda_2}$ will be approximately proportional to the acetone pressure, Eq. {5}. This will cause the type of curvature observed in the graphs. Essentially the same explanation was put forward by Oster and Marcus, who obtained similar results from irradiations with the entire flash spectrum.

In high intensity photolysis, the actual presence of an inert gas seems not to affect the production of carbon monoxide. The slightly decreased production that was observed in the present investigation when helium was added is probably an effect of the decreased reaction temperature. The effects due to inert gases reported by Roebber, Rollefson and Pimentel seem to be within the limits of experimental error. Oster and Marcus photolyzed acetone at high intensities in the presence of butane. The addition of butane decreased the ratios between the yields of ethane and carbon monoxide to values far below unity, but the carbon monoxide yields seem to have been virtually unaffected. From these data it is possible to conclude that the quantum yield of carbon monoxide production is independent of pressure and is not affected by the addition of a foreign gas in the high intensity photolysis. This conclusion would fit the theory of a dissociation from the singlet state into two methyl radicals and a carbon monoxide molecule, and is also in accordance with Heicklen's results, which showed that the fluorescence efficiency is independent of pressure [33].

The quantum yield of biacetyl was found to decrease both with increasing acetone pressure and with addition of inert gas in the investigation of Roebber, Rollefson and Pimentel [7]. This is in agreement with what has been shown in the present contribution. Heicklen observed that the phosphorescence quantum yield increased markedly with increasing acetone pressure (except at 313 mμ where a slight decrease was observed) [33]. In view of these facts, it can be concluded that excited triplet molecules, which can dissociate into acetyl and methyl radicals, lose their excess energy at the increased collision frequency obtaining at higher pressures. A unimolecular dissociation of the triplet would give a satisfactory explanation of the observed facts.

At very high light intensities, collisions between two triplet molecules and collisions between a triplet molecule and a free radical will be frequent. Very little is known about the nature of such collisions.

It may be added that Roebber, Rollefson and Pimentel suggested the following primary processes:

$$K^* \rightarrow CH_3 + CH_3CO, \tag{35}$$

$$K^* + K \rightarrow 2CH_3 + CO + K, \tag{36}$$

$$K^* + K \rightarrow K + K, \tag{37}$$

where K^* is the state formed by absorption of radiation and K the unexcited acetone molecule. The two primary processes are thus a direct dissociation of excited molecules into methyl and acetyl radicals (35), and a collision-induced dissociation into two methyl radicals and carbon monoxide (36). The excited molecule may return to the ground state in a collision with an unexcited acetone molecule (37). The mechanism was supported by the definite increase in the quantum yield of carbon monoxide with increase in pressure which they found during flash photolysis using pressures rising from 50 to 100 mm Hg. However, this mechanism has been disregarded in view of the results from other investigations [10].

Reactions involving minor dissociation products

The mechanism presented above thus accounts for the yields of ethane, carbon monoxide and biacetyl and possibly for the production of methane and acetaldehyde. The production of hydrogen and methyl ethyl ketone was not considered. In the above discussion the primary dissociation process (P15) was omitted. If process (P15) occurs, several possible reactions must be considered.

$$CH_3COCH_2 + CH_3COCH_2 \rightarrow (CH_3COCH_2)_2, \tag{38}$$

$$CH_3COCH_2 + H \rightarrow CH_3COCH_3, \tag{39}$$

$$CH_3COCH_2 + CH_3 \rightarrow CH_3COC_2H_5, \tag{40a}$$

$$CH_3COCH_2 + CH_3 \rightarrow CH_2COCH_2 + CH_4, \tag{40b}$$

$$CH_3COCH_2 + CH_3CO \rightarrow CH_3COCH_2COCH_3, \tag{41}$$

$$H + H \rightarrow H_2, \tag{42}$$

$$H + CH_3 \rightarrow CH_4, \tag{43}$$

$$H + CH_3CO \rightarrow CH_3CHO. \tag{44}$$

The reactions (38), (40a) and (41) appear in the reaction scheme given by Noyes and Dorfman [36]. The only likely source for the yield of methyl ethyl ketone which has been obtained seems to be reaction (40a). The amount of methyl ethyl ketone produced is not changed when helium is added, which supports the assumption that acetonyl radicals are formed in process (P15) and are not a product of a reaction between methyl radicals and acetone molecules, reaction (20). The fact that the yield of methyl ethyl ketone does not increase at higher acetone pressures is also in accordance with its formation at shorter wavelengths, where total absorption of the incident light is soon reached, compare Eqs. {40} and {41}. If acetonyl radicals were produced in a first order radical reaction, the relative yield of methyl ethyl ketone would show an increase with higher pressures of acetone, compare Eq. {36}. In a recent paper, Darwent, Allard, Hartman and Lange suggested that methane is formed in a disproportionation reaction between an acetonyl and a methyl radical (40b) [37].

Hydrogen atoms are produced in the primary process (P15). The reactions (39), (42), (43) and (44) must therefore be considered if hydrogen atoms are present [7]. The hydrogen atom may also abstract another hydrogen atom from an acetone molecule,

$$H + CH_3COCH_3 \rightarrow H_2 + CH_3COCH_2. \qquad (45)$$

In reactions (42) and (43), a third body is undoubtedly of importance. Methane formation by the addition of deuterium atoms to methyl radicals was shown to occur in the presence of a third body by Berisford and Le Roy [38]. Four reactions giving rise to methane have been discussed in the foregoing sections (18b), (20), (40b) and (43). It should be noted in this connection that methane was found to be a product when acetone was photolyzed in Apparatus III, where the acetone was exposed in the wavelength band around 280 mμ. In a high intensity photolysis study of acetone, Oster and Marcus found methane among the end products, even when the photolysis was undertaken in filtered light [8]. Here, use was made of a cellophane filter which absorbed most of the light below 210 mμ. Hydrogen was not found to be a product in this experiment. However, when unfiltered light was used, hydrogen was not found either. In the present investigation, the hydrogen formation decreased at higher acetone pressures, whereas the yield of methane in relation to the yield of other products increased. This might indicate that reaction (43) contributes to the methane formation.

Quantum yield

In view of the above discussion, there seem to be two possible explanations for the observed low quantum yields of formation of ethane at the high intensities used in the present investigation. These are:

1. The recombination reaction (18a) is greatly increased in relation to other reactions.

2. The triplet molecule is effectively deactivated to the ground state in collisions between two such molecules.

It seems useful to discuss these two possibilities separately, although with the information available it seems impossible to state with any certainty which of the two alternatives is the correct one.

1. The overall photolytic dissociation of acetone can be described by the following reaction

Table 7. Photolysis of acetone in Apparatus III. Determination of the quantum yield for the formation of ethane (C_2H_6).

Detector: Flame ionization.
Carrier gas: Hydrogen (H_2).
Flow rate of carrier gas: 20 cm^3 min^{-1}.
Stationary phase: Linde Molecular Sieves 5A (30–52 mesh).
Column length: 106 cm.
Column temperature: 85°C.

Flash	Actinometer decomposition (amount of Fe^{+2} ions produced) Mean value molecules $\times 10^{-15}$	Pressure of acetone before photolysis mm Hg	Dose absorbed by the sample quanta $\times 10^{-15}$	Absorbed light intensity[a] (I_a) quanta cm^{-3} $sec^{-1} \times 10^{-19}$	Amount of ethane found molecules $\times 10^{-15}$	Quantum yield of ethane formation ($\phi_{C_2H_6}$)
I	595	39	$9._1$	2.5	0.13_9	0.013
		104	$23._0$	6.0	0.21_6	0.009
		167	$35._9$	9.4	0.28_4	0.007
II	589	53	$12._0$	3.2	0.16_1	0.013
		104	$22._7$	5.9	0.23_2	0.010
		173	$36._8$	9.7	0.31_9	0.008
III	509	36	$7._2$	1.9	0.11_9	0.017
		99	$18._8$	4.9	0.18_3	0.009
		171	$31._3$	8.3	0.27_2	0.008
IV	592	45	$10._3$	2.8	0.16_6	0.016
		112	$24._5$	6.4	0.25_5	0.010
		171	$36._5$	9.6	0.30_7	0.008
V	620	45	$10._8$	2.9	0.15_5	0.014
		98	$22._4$	5.9	0.22_3	0.010
		152	$34._4$	9.0	0.28_4	0.008
VI	604	107	$24._0$	6.5	0.21_6	0.009
		107	$24._0$	6.3	0.22_7	0.009
		107	$24._0$	6.3	0.22_7	0.009

[a] Calculated by setting the flash period, τ, equal to 300 μsec (Fig. 13).

$$CH_3COCH_3 \rightarrow a_1\,CH_3 + b_1\,CH_3CO \left(+\frac{a_1 - b_1}{2}\,CO\right), \qquad (46)$$

where $a_1 \geqslant b_1$. CH_3COCH_3 can be identified with the molecule M, CH_3 with the radical R_1 and CH_3CO with the radical R_2. The derivations on page 23 can be then applied if it is assumed that the rates of reactions which are first order with respect to radical concentration are low in comparison with those of second order reactions. On the basis of the observed ratio between the yields of methane and ethane, this assumption seems to be justified. From Eqs. {20} and {21} one obtains

$$\frac{\phi_{C_2H_6}}{\phi_{CH_3COCH_3}} \geqslant \frac{k_{16}^{\frac{1}{2}}\,(k_{17a} + k_{17b})^{\frac{1}{2}}}{k_{18a} + k_{18b}}, \qquad \{42\}$$

where $\phi_{C_2H_6}$ and $\phi_{CH_3COCH_3}$ are the quantum yields of formation of the products from reactions (16) and (18a) respectively at high light intensities.

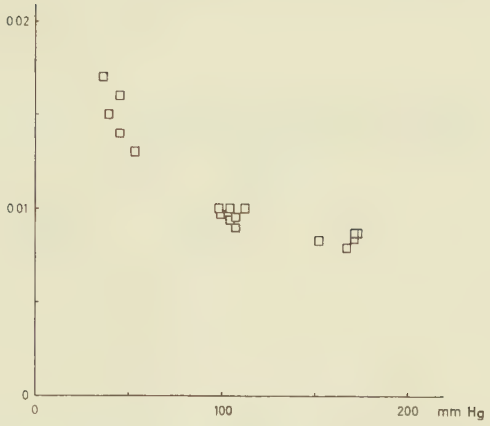

Fig. 21. Photolysis of acetone in Apparatus III. The quantum yield for the formation of ethane is plotted as a function of the acetone pressure before photolysis.

If reaction (18a) is responsible for the observed decrease in quantum yield, it follows that $(\phi_D)_l - (\phi_D)_h \leqslant \phi_{CH_3COCH_3}$, where $(\phi_D)_l$ and $(\phi_D)_h$ are the quantum yields of decomposition of acetone at low and high intensity respectively, calculated from the decomposition products. Using this condition and Eq. {42} one obtains

$$\frac{\phi_{C_2H_6}}{(\phi_D)_l - (\phi_D)_h} \geqslant \frac{k_{16}^{\frac{1}{2}}(k_{17a}+k_{17b})^{\frac{1}{2}}}{k_{18a}+k_{18b}}. \qquad \{43\}$$

The value of $(\phi_D)_l$ seems to be greater than 0.2 [3]. $\phi_{C_2H_6}$ can be taken as 0.01 from the observed quantum yield of ethane formation, Fig. 21, and a high value for $(\phi_D)_h$ is thus 0.02. It is clear then that

$$0.06 \geqslant \frac{k_{16}^{\frac{1}{2}}(k_{17a}+k_{17b})^{\frac{1}{2}}}{k_{18a}+k_{18b}}. \qquad \{44\}$$

As stated above, it is known that reaction (16) proceeds with a collision efficiency not far from unity. Therefore the rate constant k_{18a} cannot possibly be much greater than k_{16}, and it can be concluded that the rate constant $k_{17a} + k_{17b}$ must be quite small[1]. It must be remembered that this conclusion is drawn under the assumption that the reaction (18a) is responsible for the low quantum yield of ethane formation at high light intensities.

2. The expressions derived on page 25 can be applied if an efficient deactivation of the triplet molecule to the ground state in collisions between two such molecules is responsible for the low quantum yields of ethane formation at high light intensities. As the quantum yields obtained with Apparatus III have been determined using ultraviolet light of fairly long wavelength, it can be expected that the direct decomposition from the singlet will be low. If this decomposition is taken as zero, and if radical–radical reactions predominate, it seems useful to consider Eqs. {27}–{29}. In the present investigation, the absorbed intensity was varied by changing the acetone pressure, keeping the intensity of the incident light pulse the same. The

[1] $k_{18a} \approx k_{18a} + k_{18b}$.

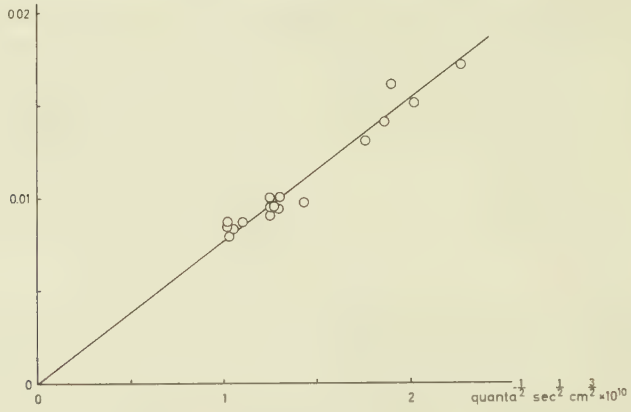

Fig. 22. Photolysis of acetone in Apparatus III. Plot of $\phi_{C_2H_6}$ (the quantum yield of ethane) as a function of $I_a^{-\frac{1}{2}}$ (the inverse square root of the absorbed intensity).

quantum yield of ethane formation was found to decrease continually as the acetone pressure was increased. Eq. {28} shows, then, that reaction (4b) cannot be the principal reaction. Furthermore, as there is no indication that the quantum yield approaches a steady value and becomes independent of intensity, it seems justifiable to disregard reaction (3b), Eq. {27}. If reaction (5b) is the predominant dissociation process, then a plot of the quantum yield of ethane as a function of the inverse square root of the absorbed intensity would give a straight line, Eq. {29}. This plot is made in Fig. 22, the values being taken from Table 7.

It is seen that the points can be satisfactorily approximated by a straight line through the origin. From the slope of the curve, it can be calculated that[1]

$$\frac{a\,k_7}{2\,k_7+\dfrac{k_8}{K_{18}}}\,\gamma^{\frac{1}{2}}\,\frac{k_{5b}}{k_{3a}^{\frac{1}{2}}}$$

for acetone has a value of 11×10^7 molecule$^{\frac{1}{2}}$ sec$^{-\frac{1}{2}}$ cm$^{-\frac{3}{2}}$.

From the above discussion, it seems reasonable to make use of the simple assumption that one triplet molecule is formed for each quantum absorbed, thus $\gamma \approx 1$. Furthermore, if it is assumed that each dissociation results in the formation of a methyl and an acetyl radical and that the methyl radicals predominantly react with each other to form ethane,

$$\frac{a\,k_7}{2\,k_7+\dfrac{k_8}{K_{18}}} \approx 0.5,$$

one obtains

[1] As reaction (3b) can be disregarded, $k_{3a}^{\frac{1}{2}} \approx (k_{3a}+k_{3b})^{\frac{1}{2}}$.

$$\frac{k_{5b}}{k_{3a}^{\frac{1}{2}}} \approx 2 \times 10^{8} \text{ molecule}^{\frac{1}{2}} \text{ sec}^{-\frac{1}{2}} \text{ cm}^{-\frac{3}{2}}. \qquad \{45\}$$

If reaction (3a) occurs at every triplet-triplet collision, a value for k_{3a} can be calculated from the classical collision theory. Taking 5 Å as the collision diameter of the triplet, one obtains the value $k_{3a} \approx 1.9 \times 10^{-10}$ cm^3 molecule^{-1} sec^{-1} at a temperature of 50°C. From Eq. {45} it can then be calculated that k_{5b} will be of the order of 3×10^3 sec^{-1}.

As reaction (4b) can be omitted, one obtains the lifetime of the phosphorescence at low light intensities from Eqs. {10} and {14} as

$$T_{\frac{1}{2}} = \frac{\ln 2}{k_{4a}[S] + k_{5a} + k_{5b}} = \frac{\phi_T \ln 2}{\gamma k_{5b}}, \qquad \{46\}$$

if reaction (5b) is the predominant dissociation process. It is known that at low intensity photolysis $0.2 \leqslant \phi_T \leqslant 1$ [3]. Using the value of k_{5b} calculated above and $\gamma = 1$, one obtains 0.5×10^{-4} sec $\leqslant T_{\frac{1}{2}} \leqslant 3 \times 10^{-4}$ sec. This agrees with the value obtained from direct measurements on the phosphorescence, 2×10^{-4} sec [34].

Acetaldehyde

Acetaldehyde was found to decompose into carbon monoxide, hydrogen, methane, ethane (Tables 8–11) and also acetone (Table 12). Analysis for formaldehyde indicated

Table 8. Photolysis of acetaldehyde in Apparatus II. Determination of the yields of methane (CH_4), and carbon monoxide (CO).

Detector: Thermal conductivity.
Carrier gas: Hydrogen (H_2).
Flow rate of carrier gas: 20 cm^3 min^{-1}.
Stationary phase: Linde Molecular Sieves 5A (30–52 mesh).
Column length: 106 cm.
Column temperature: 45°C.

Pressure of acetaldehyde before photolysis mm Hg	Yield of methane (Ψ_{CH_4}) mole × 10^8	Yield of carbon monoxide (Ψ_{CO}) mole × 10^8	$\frac{\Psi_{CH_4}}{\Psi_{CO}}$
19.0	1.7	3.2	0.53
22.0	2.1	3.5	0.60
27.1	2.9	5.0	0.58
38.9	3.7	6.4	0.58
70.1	7.1	14.4	0.49
92.8	8.3	16.3	0.51
95.0	8.8	17.0	0.52
106.6	9.0	17.9	0.50
116.9	10.7	20.8	0.51
120.0	10.5	20.1	0.52
121.0	10.6	21.3	0.50
122.8	10.2	20.7	0.49
125.1	12.5	24.9	0.50
130.0	12.1	23.4	0.52
135.2	12.4	24.8	0.50
		Mean value	0.52

Table 9. Photolysis of acetaldehyde in Apparatus II. Determination of the yield of hydrogen (H_2).

Detector: Thermal conductivity.
Carrier gas: Nitrogen (N_2).
Flow rate of carrier gas: 10 cm^3 min^{-1}.
Stationary phase: Linde Molecular Sieves 5A (30–52 mesh).
Column length: 106 cm.
Column temperature: 85°C.

Pressure of acetaldehyde before photolysis mm Hg	Yield of hydrogen (Ψ_{H_2}) mole × 10^8
20.0	1.3
30.2	1.7
39.8	1.9
50.3	2.8
51.0	2.7
76.2	4.4
90.9	4.6
98.1	4.8
110.3	5.6
114.0	5.7
127.2	7.0

Table 10. Photolysis of acetaldehyde in Apparatus II. Determination of the yields of methane (CH_4), and ethane (C_2H_6).

Detector: Flame ionization.
Carrier gas: Hydrogen (H_2).
Flow rate of carrier gas: 25 cm^3 min^{-1}.
Stationary phase: Linde Molecular Sieves 5A (30–52 mesh).
Column length: 106 cm.
Column temperature: 180°C.

Pressure of acetaldehyde before photolysis mm Hg	Yield of methane (Ψ_{CH_4}) mole × 10^8	Yield of ethane ($\Psi_{C_2H_6}$) mole × 10^8	$\frac{\Psi_{CH_4}}{\Psi_{C_2H_6}}$
32.0	3.2	1.62	2.0
33.9	3.2	1.69	1.9
78.9	7.9	3.54	2.2
		Mean value	2.0

that it might be present among the products, although quantitative measurements for this compound were not successful. They showed, however, that the amounts formed are not greater than 0.1×10^{-8} mole. It was also found that biacetyl and glyoxal are not formed in quantities exceeding 0.1×10^{-8} mole. Product yields are plotted versus pressure of acetaldehyde in Fig. 23, where it can be seen that the product yields are directly proportional to acetaldehyde pressure. The decomposition can be described by the equations

Table 11. Photolysis of acetaldehyde in Apparatus II. Determination of the yields of methane (CH_4), and ethane (C_2H_6).

Detector: Flame ionization.
Carrier gas: Hydrogen (H_2).
Flow rate of carrier gas: 20 cm^3 min^{-1}.
Stationary phase: Perkin-Elmer F (tetra ethylene glycol dimethyl ether).
Column length: 106 cm.
Column temperature: 23°C.

Pressure of acetaldehyde before photolysis mm Hg	Yield of methane (Ψ_{CH_4}) mole × 10^8	Yield of ethane ($\Psi_{C_2H_6}$) mole × 10^8	$\frac{\Psi_{CH_4}}{\Psi_{C_2H_6}}$
29.8	2.62	1.34	2.0
39.0	3.55	1.86	1.9
112.3	10.7	4.73	2.3
150.5	13.5	5.98	2.3
150.6	14.3	6.21	2.3
		Mean value	2.2

Table 12. Photolysis of acetaldehyde in Apparatus II. Determination of the yield of acetone (CH_3COCH_3).

Detector: Flame ionization.
Carrier gas: Hydrogen (H_2).
Flow rate of carrier gas: 30 cm^3 min^{-1}.
Stationary phase: Perkin-Elmer F (tetra ethylene glycol dimethyl ether).
Column length: 52 cm.
Column temperature: 22°C and 60°C.[a]

Pressure of acetaldehyde before photolysis mm Hg	Yield of acetone ($\Psi_{CH_3COCH_3}$) mole × 10^8
67.1	1.01
67.1	0.96
100.1	1.39
100.2	1.45
100.4	1.42
19.8	0.27
30.0	0.41
30.2	0.42
52.0	0.80
52.5	0.71
66.9	1.04
99.7	1.35

[a] The analyses in the first section of the table are made with a column temperature of 22°C and those in the later section at 60°C.

$$CH_3CHO = CH_4 + CO, \quad \text{(a)}$$

$$CH_3CHO = \tfrac{1}{2}C_2H_6 + \tfrac{1}{2}H_2 + CO, \quad \text{(b)}$$

$$CH_3CHO = \tfrac{1}{2}CH_3COCH_3 + \tfrac{1}{2}H_2 + \tfrac{1}{2}CO. \quad \text{(c)}$$

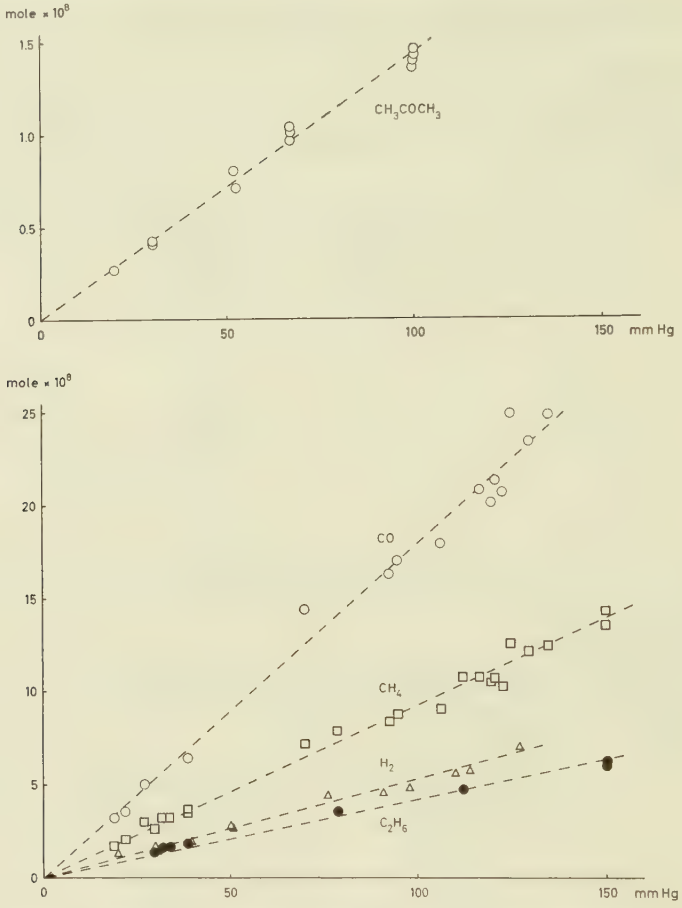

Fig. 23. Photolysis of acetaldehyde in Apparatus II. Product yields are plotted as a function of the pressure of acetaldehyde before photolysis.

Using the yields of methane, ethane and acetone, it is calculated from the curves in Fig. 23 that the equations (a)-(c) have the relative importance (a) 45 %, (b) 41 %, and (c) 14 %.

Mass balance

From the straight lines in Fig. 23, the mole ratios for the products are

$$\frac{H}{C} = 2.05 \quad \frac{O}{C} = 0.48.$$

There is thus excellent agreement with the mole ratios for acetaldehyde,

$$\frac{H}{C} = 2.00 \quad \frac{O}{C} = 0.50,$$

which supports the assumption that all important products have been recorded.

Primary processes

The primary process in the photolysis of acetaldehyde seems to be analogous to that of acetone. Murad studied the fluorescence of acetaldehyde vapour and suggested the following mechanism [39].

(47) An excited singlet in an upper vibrational level is produced when a quantum is absorbed

$$A + h\nu \rightarrow A_n^1. \tag{47}$$

This excited singlet may then react according to the following scheme:

$$A_n^1 + A \rightarrow A_o^1 + A, \tag{48}$$

$$A_n^1 \rightarrow \text{Decomposition}, \tag{49}$$

$$A_o^1 \rightarrow A + h\nu_3, \tag{50}$$

where A_o^1 represents an excited singlet in the lowest vibrational level and $h\nu_3$ the fluorescence. A triplet state is also predicted, but as no phosphorescence is observed, this triplet would have to disappear by internal conversion. The evidence for the existence of a triplet comes from the fact that phosphorescence of biacetyl can be sensitized by acetaldehyde. Nothing is known about the lifetime of either the postulated triplet or the excited singlet.

Two processes have been generally accepted to constitute the primary chemical act.

(P51) A dissociation into a methyl radical and a formyl radical.

(P52) A molecular rearrangement to form a methane molecule and a carbon monoxide molecule.

$$CH_3CHO + h\nu \rightarrow CH_3 + CHO, \tag{P51}$$

$$CH_3CHO + h\nu \rightarrow CH_4 + CO. \tag{P52}$$

There is disagreement about the relative importance of the reactions (P51) and (P52) at different wavelengths [3]. However, detailed work by Blacet and co-workers indicated that at 313 mμ the primary chemical act consists solely of reaction (P51) and that the quantum yield is low at moderate temperature [40, 41]. It is interesting to note that Lossing has shown that in the mercury photosensitized decomposition of acetaldehyde at 55°C, the primary step consists to at least 95% in the formation of methyl and formyl radicals [42]. It is known that the efficiency of reaction (P52) increases at shorter wavelengths.

Khan, Norrish and Porter found acetone as a product of the high intensity photolysis of acetaldehyde and to account for this they adopted the primary dissociation (P53), which produced an acetyl radical and a hydrogen atom

$$CH_3CHO + h\nu \rightarrow CH_3CO + H. \tag{P53}$$

Radical reactions

Possible reactions between methyl radicals and formyl radicals that have been postulated are

$$CH_3 + CH_3 \rightarrow C_2H_6, \quad (16)$$

$$CHO + CHO \rightarrow (CHO)_2, \quad (54a)$$

$$CHO + CHO \rightarrow H_2 + 2\,CO, \quad (54b)$$

$$CHO + CHO \rightarrow CO + HCHO, \quad (54c)$$

$$CH_3 + CHO \rightarrow CH_3CHO, \quad (55a)$$

$$CH_3 + CHO \rightarrow CH_4 + CO. \quad (55b)$$

Two reactions which are first order with respect to radical concentration should be considered. These are the decomposition of the formyl radical and the reaction of methyl radicals with acetaldehyde molecules. These reactions are discussed in a separate section on page 65. For convenience, the reaction between methyl radicals and acetaldehyde, which produces methane and acetyl radicals, is given below

$$CH_3 + CH_3CHO \rightarrow CH_4 + CH_3CO. \quad (56)$$

Reaction (16) was discussed when dealing with the photolysis of acetone, page 31.

There are three possible reactions which may occur when two formyl radicals collide. Both glyoxal and formaldehyde have been found to be products of the photolysis of acetaldehyde using low light intensities [43]. Their formation in a homogeneous reaction of two formyl radicals cannot, however, be important in view of the absence from the products of appreciable quantities of these compounds in the present investigation. Reaction (54b) seems to be the actual reaction and appears in the scheme given by Khan, Norrish and Porter [5].

Mains, Roebber and Rollefson discussed the reaction of a methyl and a formyl radical and concluded that this reaction principally involved a recombination to form acetaldehyde [6]. This is not in agreement with the results obtained in the present investigation from the photolysis of propionaldehyde, see page 56. These results showed that reaction (55b) is the predominant reaction. This is also in accordance with the conclusion made by Lossing from a mass spectrometry study of the mercury photosensitized decomposition of acetaldehyde [42]. Lossing concluded that at 55°C and low pressures, reaction (55b) must be at least as fast as the combination of methyl radicals to form ethane, reaction (16). Furthermore, Blake and Kutschke deduced from a study of the reaction of methyl radicals with formaldehyde that the value of $k_{55b}/(k_{55a} + k_{55b})$ is close to unity [44].

There seems to be no doubt that the acetone which has been found arises in a reaction between a methyl and an acetyl radical

$$CH_3 + CH_3CO \rightarrow CH_3COCH_3. \quad (18a)$$

Acetyl iodide has not been detected as a product of the photolysis of acetaldehyde-iodine mixtures, which finding argues against the acetyl radical being formed in reaction (P53) [3]. The photolysis studies with Apparatus II showed, however, that acetone represents a constant fraction of the other products when the acetaldehyde pressure is varied. This fact indicates that acetyl radicals are not formed in a reaction which is first order with respect to radical concentration, compare Eq. {36}.

Propionaldehyde

The main products from the photolysis of propionaldehyde in Apparatus II were found to be carbon monoxide, hydrogen, ethane and butane. Considerable amounts of methane, ethylene and propane are also found (Tables 13–17). Acetaldehyde is not present in the end products in amounts exceeding 0.01×10^{-8} mole. Products are arranged versus pressure in Fig. 24.

If no other products than these recorded are formed, then the overall decomposition can be represented stoichiometrically by the following five equations (the possible existence of formaldehyde being neglected):

$$C_2H_5CHO = C_2H_6 + CO, \quad \text{(d)}$$

$$C_2H_5CHO = \tfrac{1}{2}C_4H_{10} + \tfrac{1}{2}H_2 + CO, \quad \text{(e)}$$

$$C_2H_5CHO = \tfrac{2}{3}C_3H_8 + \tfrac{1}{3}H_2 + CO, \quad \text{(f)}$$

$$C_2H_5CHO = C_2H_4 + H_2 + CO, \quad \text{(g)}$$

$$C_2H_5CHO = 2CH_4 - H_2 + CO. \quad \text{(h)}$$

Table 13. Photolysis of propionaldehyde in Apparatus II. Determination of the yield of carbon monoxide (CO).

Detector: Thermal conductivity.
Carrier gas: Hydrogen (H_2).
Flow rate of carrier gas: 20 cm^3 min^{-1}.
Stationary phase: Linde Molecular Sieves 5A (30–52 mesh).
Column length: 106 cm.
Column temperature: 45°C and 50°C.[a]

Pressure of propionaldehyde before photolysis mm Hg	Yield of carbon monoxide (Ψ_{CO}) mole $\times 10^8$
9.2	3.0
11.1	4.4
11.2	4.0
20.9	9.3
20.9	9.0
21.0	9.0
31.1	11.7
31.3	11.4
60.0	25.5
60.0	27.3
100.2	33.8
100.3	35.5
14.7	6.7
15.9	7.9
40.1	19.1
45.0	20.1
55.0	21.6
77.5	31.0
82.5	32.5

[a] The analyses in the first section of the table are made with a column temperature of 45°C and those in the later section at 50°C.

Table 14. Photolysis of propionaldehyde in Apparatus II. Determination of the yield of hydrogen (H_2).

Detector: Thermal conductivity.
Carrier gas: Nitrogen (N_2).
Flow rate of carrier gas: 10 cm^3 min^{-1}.
Stationary phase: Linde Molecular Sieves 5A (30–52 mesh).
Column length: 106 cm.
Column temperature: 30°C.

Pressure of propionaldehyde before photolysis mm Hg	Yield of hydrogen (Ψ_{H_2}) mole × 10^8
30.1	3.7
30.2	3.3
50.1	4.8
50.3	5.7
61.0	6.1
61.2	6.1
83.9	8.3
84.3	8.0
99.0	9.1
100.4	9.1

The values for the hydrocarbon yields from the photolysis of propionaldehyde can be obtained from the graphs in Fig. 24. Using these values, and taking the propionaldehyde pressure to be 50 mm Hg, the relative importance of the decompositions (d)–(h) is calculated to be (d) 51 %, (e) 37 %, (f) 6.6 %, (g) 4.6 %, and (h) 1.2 %.

Mass balance

The products show the following mole ratios:

$$\frac{H}{C} = 2.02 \quad \frac{O}{C} = 0.32.$$

The values for propionaldehyde are

$$\frac{H}{C} = 2.00 \quad \frac{O}{C} = 0.33.$$

The discrepancy is thus very low, indicating that the recorded products give a full account of the process.

Primary processes

Four reactions have been proposed to constitute the primary chemical act in the photolysis of propionaldehyde [45].

$$C_2H_5CHO + h\nu \rightarrow C_2H_5 + CHO, \qquad (P57)$$

$$C_2H_5CHO + h\nu \rightarrow C_2H_6 + CO, \qquad (P58)$$

Table 15. Photolysis of propionaldehyde in Apparatus II. Determination of the yields of methane (CH_4), and ethane (C_2H_6).

Detector: Flame ionization.
Carrier gas: Hydrogen (H_2).
Flow rate of carrier gas: 25 cm^3 min^{-1}.
Stationary phase: Linde Molecular Sieves 5A (30–52 mesh).
Column length: 106 cm.
Column temperature: 180°C.

Pressure of propionaldehyde before photolysis mm Hg	Yield of methane (Ψ_{CH_4}) mole × 10^8	Yield of ethane ($\Psi_{C_2H_6}$) mole × 10^8	$\frac{\Psi_{CH_4}}{\Psi_{C_2H_6}}$
46.2	0.47	9.4	0.050
50.1	0.52	11.5	0.045
50.3	0.58	11.2	0.052
		Mean value	0.049

Table 16. Photolysis of propionaldehyde in Apparatus II. Determination of the yields of methane (CH_4), ethane (C_2H_6), and ethylene (C_2H_4).

Detector: Flame ionization.
Carrier gas: Hydrogen (H_2).
Flow rate of carrier gas: 25 cm^3 min^{-1}.
Stationary phase: Linde Molecular Sieves 5A (30–52 mesh).
Column length: 106 cm.
Column temperature: 200°C.

Pressure of propionaldehyde before photolysis mm Hg	Yield of methane (Ψ_{CH_4}) mole × 10^8	Yield of ethane ($\Psi_{C_2H_6}$) mole × 10^8	Yield of ethylene ($\Psi_{C_2H_4}$) mole × 10^8	$\frac{\Psi_{CH_4}}{\Psi_{C_2H_6}}$	$\frac{\Psi_{C_2H_4}}{\Psi_{C_2H_6}}$
45.8	0.47	10.4	1.06	0.045	0.102
52.0	0.45	12.0	0.89	0.038	0.074
75.8	0.77	15.4	1.24	0.050	0.081
20.3	0.22	4.3	0.39	0.051	0.091
23.2	0.22	5.1	0.53	0.043	0.104
23.5	0.26	5.0	0.47	0.052	0.094
48.3	0.53	10.3	1.05	0.051	0.102
50.0	0.46	11.7	1.07	0.039	0.091
95.8	0.83	18.2	1.74	0.046	0.096
96.1	0.84	19.3	1.80	0.044	0.093
97.0	0.91	19.1	1.69	0.048	0.088
97.0	0.81	19.1	1.82	0.042	0.095
			Mean value	0.046	0.093

$$C_2H_5CHO + h\nu \rightarrow C_2H_4 + HCHO, \qquad (P59)$$

$$C_2H_5CHO + h\nu \rightarrow CH_3 + CH_2CHO. \qquad (P60)$$

Blacet and Pitts concluded that at 313 mμ reaction (P57) is highly favoured, but at 265 mμ reactions (P57) and (P58) are equally probable [45]. Furthermore, they

Table 17. Photolysis of propionaldehyde in Apparatus II. Determination of the yields of ethane (C_2H_6) + ethylene (C_2H_4), propane (C_3H_8), and *n*-butane (C_4H_{10}).

Detector: Flame ionization.
Carrier gas: Hydrogen (H_2).
Flow rate of carrier gas: 30 cm^3 min^{-1}.
Stationary phase: Perkin-Elmer D (tetraisobutylene).
Column length: 106 cm.
Column temperature: 23°C.

Pressure of propionaldehyde before photolysis mm Hg	Yield of ethane + ethylene ($\Psi'_{C_2H_6+C_2H_4}$) mole × 10^8	Yield of propane ($\Psi'_{C_3H_8}$) mole × 10^8	Yield of *n*-butane ($\Psi'_{C_4H_{10}}$) mole × 10^8	$\frac{\Psi'_{C_2H_6+C_2H_4}}{\Psi'_{C_4H_{10}}}$	$\frac{\Psi'_{C_3H_8}}{\Psi'_{C_4H_{10}}}$
42.0	10.0	0.83	3.39	2.0	0.24
42.1	10.7	1.01	3.44	3.1	0.29
60.2	13.9	1.22	5.01	2.8	0.24
69.9	13.7	1.16	5.25	2.6	0.22
70.3	14.6	1.19	5.56	2.6	0.21
75.9	14.9	1.31	5.34	2.8	0.25
100.0	18.7	1.48	8.11	2.3	0.18
110.3	19.8	1.49	8.97	2.2	0.17
110.5	19.3	1.49	8.25	2.3	0.18
25.2	6.0	0.54	1.90	3.2	0.28
25.7	6.4	0.50	1.92	3.3	0.26
29.3	6.7	0.54	2.61	2.6	0.21
80.1	16.6	1.37	6.13	2.7	0.22
82.4	17.2	1.64	6.74	2.6	0.24
83.0	16.1	1.69	6.78	2.4	0.25
89.9	18.4	1.77	6.82	2.7	0.26
97.2	19.4	1.74	7.71	2.5	0.23
			Mean value	2.7	0.23

stated that process (P60) is negligible at 313 mμ but not at 238 mμ, whereas reaction (P59) is of minor importance at all wavelengths. These results are based on experiments performed on mixtures of propionaldehyde and iodine. Doubt has been expressed about the validity of some of the deductions regarding free radical mechanism based on the use of iodine, as the presence of iodine will undoubtedly quench some of the electronically-excited states formed.

Radical reactions

If only reactions which are second order with respect to radicals are considered, the following reaction scheme can be postulated:

$$C_2H_5 + C_2H_5 \rightarrow C_4H_{10}, \quad (61a)$$

$$C_2H_5 + C_2H_5 \rightarrow C_2H_6 + C_2H_4, \quad (61b)$$

$$CHO + CHO \rightarrow H_2 + 2CO, \quad (54b)$$

$$C_2H_5 + CHO \rightarrow C_2H_5CHO, \quad (62a)$$

$$C_2H_5 + CHO \rightarrow C_2H_6 + CO, \quad (62b)$$

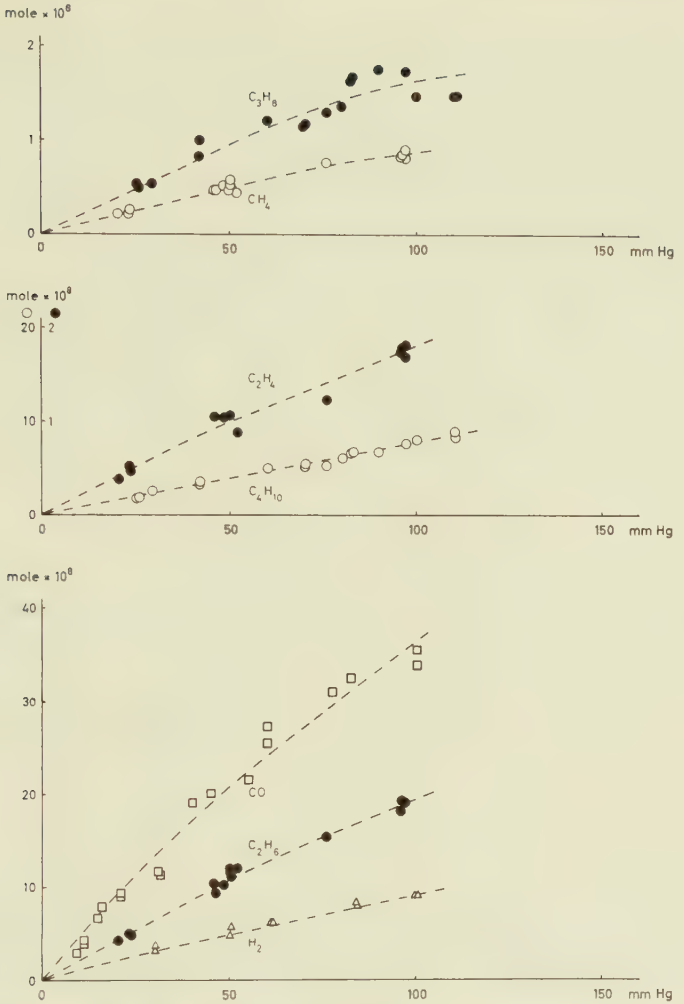

Fig. 24. Photolysis of propionaldehyde in Apparatus II. Product yields are plotted as a function of the pressure of propionaldehyde before photolysis.

$$C_2H_5 + CH_3 \rightarrow C_3H_8, \quad (63a)$$

$$C_2H_5 + CH_3 \rightarrow C_2H_4 + CH_4, \quad (63b)$$

$$CH_3 + CHO \rightarrow CH_3CHO, \quad (55a)$$

$$CH_3 + CHO \rightarrow CH_4 + CO, \quad (55b)$$

$$CH_3 + CH_3 \rightarrow C_2H_6. \quad (16)$$

Little seems to be known about the reactions of the radical CH_2CHO. As the primary process (P60) represents only a small fraction of the total decomposition, it is difficult to obtain any information about the participation of this radical in secondary reactions. It has therefore not been included in the scheme.

It is thought that reactions which are first order with respect to radical concentration are of minor importance, as the ratio between any two products has been found to remain constant when the propionaldehyde pressure was varied, compare Eq. {36}. These reactions are discussed on page 65.

Reaction (61a) provides the only source of *n*-butane. Using a sector technique, Shepp and Kutschke calculated that $\log k_{61a} = 14.5 - 2000/2.303\,\boldsymbol{R}T$ [46]. The rate constant is then expressed in $cm^3\ mole^{-1}\ sec^{-1}$. It has been argued, however, that the temperature coefficient possibly has no real significance [47]. Reaction (61b) involves the disproportionation of ethyl radicals. Values of k_{61b}/k_{61a} have been reported in the literature. According to these reports, k_{61b}/k_{61a} remains constant over a wide temperature range, which means that the activation energy of reactions (61a) and (61b) is the same. The agreement between the results of various investigations seems to be fairly good. A value of 0.15 ± 0.01 for k_{61b}/k_{61a} was reported by Smith, Beatty, Pinder and Le Roy, who studied the mercury photosensitized hydrogenation of ethylene [48]. On the other hand, Brinton and Steacie arrived at a value of 0.12 from a study of the photolysis of diethyl ketone at low pressures [49]. Mass-spectrometric analysis of the products from photolysis of diethyl ketone has given the value of 0.136 ± 0.02, as reported by James and Steacie [50]. From a photolysis study of propionaldehyde, Kerr and Trotman-Dickenson obtained the value 0.150 [47].

The reaction caused by a collision of two formyl radicals is described by reaction (54b). The importance of other reactions was discussed when dealing with the scheme of acetaldehyde photolysis, page 50.

The reaction of an ethyl radical and a formyl radical may involve a recombination (62a) or a formation of ethane and carbon monoxide (62b). The parallel with reaction (55b), which is discussed later, suggests that reaction (62b) is the important step.

The ratio of the rate constants for disproportionation and combination in a reaction between an ethyl radical and a methyl radical, i.e. k_{63b}/k_{63a}, has been determined by Heller, who found a value of 0.06 ± 0.01 from a mass-spectrometric study [51]. Reaction (63a) seems to provide the only possible source for the formation of propane, while the ratio between the yields of methane and propane found in the present investigation is much higher than 0.06. This indicates that methane must also arise in another reaction than (63b), which it is seen to do in reaction (55b) of the postulated scheme. Acetaldehyde is found to be absent in the products from propionaldehyde photolysis. This implies that a reaction between a methyl radical and a formyl radical preferentially takes the course of (55b) to form methane and carbon monoxide.

In view of the discussion given above, several reactions can be excluded from the scheme for propionaldehyde, which in its simplified form contains the reactions (61a), (61b), (62b), (63a), (63b), (54b), (55b) and (16). The various products, and the reactions which give rise to them, are tabulated below.

Product	Reactions in which the product is formed	Amount of product formed in photolysis at 50 mm Hg pressure mole × 10^8
C_4H_{10}	(61a)	4.0
C_3H_8	(63a)	0.95
H_2	(54b)	5.0
CH_4	(63b) + (55b)	0.50
C_2H_4	(61b) + (63b) + (P 59)	1.00
C_2H_6	(61b) + (62b) + (16) + (P 58)	11.0
CO	(62b) + (54b) + (55b) + (P 58)	20.7

The last column shows the amounts of products which were found experimentally to be obtained when propionaldehyde was photolyzed at a pressure of 50 mm Hg. The values are taken from the graphs in Fig. 24.

By using this simplified scheme, the relative importance of the reactions can be determined by making use of the amounts of products formed and of the values of k_{61b}/k_{61a} and k_{63b}/k_{63a} (0.15 and 0.06 respectively). From the quantities of butane, propane, hydrogen, methane and ethylene, the following reaction yields are obtained: (61a) 4.0×10^{-8} mole, (61b) 0.60×10^{-8} mole, (63a) 0.95×10^{-8} mole, (63b) 0.06×10^{-8} mole, (54b) 5.0×10^{-8} mole, (55b) 0.44×10^{-8} mole, and (P59) 0.34×10^{-8} mole. When considering these values, it should be remembered that the participation of the radical CH_2CHO in the reactions has been neglected.

The quantities of ethane and carbon monoxide give the relations: yield of (P58) + (62b) + (16) equal to 10.4×10^{-8} mole, yield of (P58) + (62b) equal to 10.3×10^{-8} mole. The contribution of reaction (16) must be very small, and it is thus clear that the reaction scheme satisfies the experimentally determined data.

n-Butyraldehyde

It is observed from Tables 18–21 that the main components among the products in the photolysis of *n*-butyraldehyde in Apparatus II are carbon monoxide, acetaldehyde, hydrogen, ethylene, propane, propylene and *n*-hexane. As can be seen from the tables, trace quantities of butane and pentane have also been found to be present.

Neglecting the trace components, the analytical results can be described by the following four equations:

$$C_3H_7CHO = C_2H_4 + CH_3CHO, \quad \text{(i)}$$

$$C_3H_7CHO = C_3H_8 + CO, \quad \text{(j)}$$

$$C_3H_7CHO = \tfrac{1}{2}C_6H_{14} + \tfrac{1}{2}H_2 + CO, \quad \text{(k)}$$

$$C_3H_7CHO = C_3H_6 + H_2 + CO. \quad \text{(l)}$$

Experimentally, a slight difference is observed in the yield of ethylene and acetaldehyde. In view of the following discussion it seems, however, convenient to equalize the yields of ethylene and acetaldehyde stoichiometrically. From the observed hydrocarbon yields, the relative significances of the decompositions (i)–(l) are (i) 50%, (j) 22%, (k) 25%, and (l) 2.7%.

Mass balance

The mole ratios for the products calculated from the mean values in Tables 18, 19 and 21 are found to be

$$\frac{H}{C} = 2.01 \quad \frac{O}{C} = 0.24.$$

These values should be compared with

$$\frac{H}{C} = 2.00 \quad \frac{O}{C} = 0.25$$

for the butyraldehyde molecule.

Table 18. Photolysis of *n*-butyraldehyde in Apparatus II. Determination of the yield of carbon monoxide (CO).

Detector: Thermal conductivity.
Carrier gas: Hydrogen (H_2).
Flow rate of carrier gas: 20 cm^3 min^{-1}.
Stationary phase: Linde Molecular Sieves 5A (30–52 mesh).
Column length: 106 cm.
Column temperature: 45°C.

Pressure of *n*-butyraldehyde before photolysis mm Hg		Yield of carbon monoxide (Ψ_{CO}) mole × 10^8
30.1		1.76
30.2		1.71
30.4		1.83
30.4		1.81
30.4		1.68
	Mean value	1.76
11.0		0.39
11.1		0.37
21.0		0.81
21.0		1.04
21.2		0.99
30.8		1.85
30.9		1.78
40.9		2.64
40.9		2.81
41.2		2.72

Primary processes

The primary decomposition in the photolysis of *n*-butyraldehyde has been described to consist of the following four reactions [52, 53]:

$$C_3H_7CHO + h\nu \rightarrow C_3H_7 + CHO, \quad \text{(P64)}$$

$$C_3H_7CHO + h\nu \rightarrow C_3H_8 + CO, \quad \text{(P65)}$$

$$C_3H_7CHO + h\nu \rightarrow C_2H_4 + CH_3CHO, \quad \text{(P66)}$$

$$C_3H_7CHO + h\nu \rightarrow CH_3 + C_2H_4CHO. \quad \text{(P67)}$$

C_3H_7 symbolizes in connection with *n*-butyraldehyde the *n*-propyl radical.

By photolyzing *n*-butyraldehyde in the presence of iodine, Blacet and Calvert estimated the quantum yields of the different primary processes at various wavelengths [53]. They concluded that reaction (P64) is important at all the wavelengths investigated (253.7–313 mμ), whereas reaction (P65) is only of importance at the shorter wavelengths within this range. Similarly, reaction (P66) was found to be important at all these wavelengths and reaction (P67) only at the shorter wavelengths. However, as it has been argued that a selective de-activation of the excited butyraldehyde molecule by the heavy iodine atoms may occur, the validity of the values given

Table 19. Photolysis of *n*-butyraldehyde in Apparatus II. Determination of the yield of hydrogen (H_2).

Detector: Thermal conductivity.
Carrier gas: Nitrogen (N_2).
Flow rate of carrier gas: 10 cm^3 min^{-1},
Stationary phase: Linde Molecular Sieves 5A (30–52 mesh).
Column length: 106 cm.
Column temperature: 30°C.

Pressure of *n*-butyraldehyde before photolysis mm Hg	Yield of hydrogen (Ψ_{H_2}) mole × 10^8
30.1	0.59
30.3	0.56
30.3	0.49
30.3	0.56
30.4	0.51
Mean value	0.54

Table 20. Photolysis of *n*-butyraldehyde in Apparatus II. Determination of the yields of ethylene (C_2H_4), propane (C_3H_8) + propylene (C_3H_6), and acetaldehyde (CH_3CHO).

Detector: Flame ionization.
Carrier gas: Hydrogen (H_2).
Flow rate of carrier gas: 30 cm^3 min^{-1}.
Stationary phase: Perkin-Elmer D (Tetraisobutylene).
Column length: 106 cm.
Column temperature: 23°C.

Pressure of *n*-butyraldehyde before photolysis	Yield of ethylene ($\Psi_{C_2H_4}$) mole × 10^8	Yield of propane + propylene ($\Psi_{C_3H_8+C_3H_6}$) mole × 10^8	Yield of acetaldehyde (Ψ_{CH_3CHO}) mole × 10^8	$\frac{\Psi_{C_3H_8+C_3H_6}}{\Psi_{C_2H_4}}$	$\frac{\Psi_{CH_3CHO}}{\Psi_{C_2H_4}}$
29.7	1.81	0.85	1.6	0.47	0.88
29.9	1.86	0.93	1.8	0.50	0.97
30.0	1.76	0.91	1.7	0.52	0.97
30.1	1.83	0.93	1.8	0.51	0.98
30.3	1.88	0.95	1.8	0.51	0.96
30.3	1.88	0.89	1.8	0.47	0.96
Mean value	1.84	0.91	1.8	0.50	0.95

by Blacet and Calvert seems somewhat doubtful. It should be noted that Kerr and Trotman-Dickenson write primary process (P68) instead of process (P67) [54].

$$C_3H_7CHO + h\nu \rightarrow CH_3 + C_2H_4 + CHO. \qquad (P68)$$

Radical reactions

On the basis of the results of earlier work and of those of the present investigation, the following reaction scheme will serve as a useful framework for the interpretation of the results:

Table 21. Photolysis of *n*-butyraldehyde in Apparatus II. Determination of the yields of ethylene (C_2H_4), propane (C_3H_8), propylene (C_3H_6), *n*-butane (C_4H_{10}), *n*-pentane (C_5H_{12}), *n*-hexane (C_6H_{14}), and acetaldehyde (CH_3CHO).

Detector: Flame ionization.
Carrier gas: Hydrogen (H_2).
Flow rate of carrier gas: 20 cm^3 min^{-1}.
Stationary phase: Perkin-Elmer F (tetra ethylene glycol dimethyl ether).
Column length: 106 cm.
Column temperature: 22°C.

Flash	Pressure of *n*-butyraldehyde before photolysis mm Hg	Yield of ethylene ($\Psi'_{C_2H_4}$) mole × 10^8	Yield of propane ($\Psi'_{C_3H_8}$) mole × 10^8	Yield of propylene ($\Psi'_{C_3H_6}$) mole × 10^8	Yield of *n*-butane ($\Psi'_{C_4H_{10}}$) mole × 10^8	Yield of *n*-pentane ($\Psi'_{C_5H_{12}}$) mole × 10^8	Yield of *n*-hexane ($\Psi'_{C_6H_{14}}$) mole × 10^8	Yield of acetaldehyde (Ψ'_{CH_3CHO}) mole × 10^8
I	30.0	1.89	0.81	0.10	0.03	0.02	0.44	1.66
II	30.1	1.81	0.75	0.10	0.03	0.02	0.42	1.80
III	30.1	1.76	0.73	0.09	0.02	0.02	0.48	1.70
IV	30.2	1.93	0.86	0.11	0.03	0.03	0.50	1.84
V	30.3	1.88	0.83	0.10	0.03	0.02	0.48	1.68
	Mean value	1.85	0.80	0.10	0.03	0.02	0.46	1.74

Flash	$\frac{\Psi'_{C_2H_8}}{\Psi'_{C_2H_4}}$	$\frac{\Psi'_{C_3H_6}}{\Psi'_{C_2H_4}}$	$\frac{\Psi'_{C_4H_{10}}}{\Psi'_{C_2H_4}}$	$\frac{\Psi'_{C_5H_{12}}}{\Psi'_{C_2H_4}}$	$\frac{\Psi'_{C_6H_{14}}}{\Psi'_{C_2H_4}}$	$\frac{\Psi'_{CH_3CHO}}{\Psi'_{C_2H_4}}$
I	0.43	0.05_3	0.02	0.01	0.23	0.88
II	0.41	0.05_5	0.02	0.01	0.23	0.99
III	0.41	0.05_1	0.01	0.01	0.27	0.97
IV	0.45	0.05_7	0.02	0.02	0.26	0.95
V	0.44	0.05_3	0.02	0.01	0.26	0.89
Mean value	0.43	0.05_4	0.02	0.01	0.25	0.94

$$C_3H_7 + C_3H_7 \rightarrow C_6H_{14}, \quad (69a)$$

$$C_3H_7 + C_3H_7 \rightarrow C_3H_8 + C_3H_6, \quad (69b)$$

$$CHO + CHO \rightarrow H_2 + 2CO, \quad (54b)$$

$$C_3H_7 + CHO \rightarrow C_3H_7CHO, \quad (70a)$$

$$C_3H_7 + CHO \rightarrow C_3H_8 + CO, \quad (70b)$$

$$C_3H_7 + CH_3 \rightarrow C_4H_{10}, \quad (71a)$$

$$C_3H_7 + CH_3 \rightarrow C_3H_6 + CH_4, \quad (71b)$$

$$CH_3 + CHO \rightarrow CH_4 + CO, \quad (55b)$$

$$CH_3 + CH_3 \rightarrow C_2H_6. \quad (16)$$

The possible existence of the radical C_2H_4CHO and its reactions are neglected in the scheme, as this radical only occurs in small quantities and nothing is known of the nature of its participation in secondary reactions.

Reactions which are first order with respect to radical concentration are discussed on page 65. Their importance seems to be slight.

The rate constant for the recombination of two *n*-propyl radicals, k_{69a}, was measured by Whiteway and Masson [55]. They studied the photolysis of di-*n*-propyl ketone in intermittent light and obtained a value of $k_{69a} = 1 \times 10^{-8}$ cm^3 molecule^{-1} sec^{-1} at 100°C. However, as this experimental value is much higher than that expected on the basis of a reaction occurring at every classical collision, they concluded that it was probably too high by a factor of 20. There is little agreement concerning the value of k_{69b}/k_{69a}. Caule and Steacie found the value 0.3 [56]. Blacet and Calvert estimated k_{69b}/k_{69a} to be 0.1 from a photolysis study of *n*-butyraldehyde at room temperature [53]. Masson investigated the photolysis of di-*n*-propyl ketone and found $k_{69b}\ k_{69a} = 0.20$ at 113°C [57]. In the investigation by Whiteway and Masson, the most probable value of k_{69b}/k_{69a} was estimated to be 0.125 [55]. They concluded that there is zero difference in activation energy between reactions (69a) and (69b). Kerr and Trotman-Dickenson investigated the ratio k_{69b}/k_{69a} over a wide temperature range and give a constant value of 0.16 [54]. The reaction scheme above provides one source for *n*-hexane, reaction (69a), and two sources for propylene, reactions (69b) and (71b). From the mean values of the yields of *n*-hexane and propylene in Table 21 we thus get

$$\frac{k_{69b}}{k_{69a}} \leqslant 0.22. \quad \{47\}$$

The contribution to the propylene production from reaction (71b) is probably small in view of the low yield of butane from reaction (71a). The ratio k_{71b}/k_{71a} is not known, but is probably less than unity. Consequently the value 0.2 for k_{69b}/k_{69a} can be given.

Reactions (54b), (55b) and (16) were discussed on pages 50 and 31 respectively.

The results obtained do not enable the relative importance of reactions (70a) and (70b) to be determined. The parallel with reaction (55b), which was discussed on pages 50 and 56, suggests that reaction (70b) is the important step.

The ethylene yields are somewhat higher than the acetaldehyde yields, which may be due to experimental error. The possible yield of ethylene from the process

(P67, P68) is probably of little importance in view of the small yield of products from reactions involving methyl radicals. Trace quantities of pentane are formed, but there is too little information available to predict the source of this pentane with any certainty. The possibility that ethyl radicals, which can form pentane together with propyl radicals, are produced in a primary process should, however, not be excluded. The possibility of pentane formation in a reaction between propyl radicals and the radical C_2H_4CHO should also be investigated.

Isobutyraldehyde

Carbon monoxide, hydrogen, propane, propylene and di-isopropyl have been found to be the products of the photolysis of isobutyraldehyde (Tables 22–24). Analysis for methane showed that this substance cannot be present in quantities exceeding 0.01×10^{-8} mole. The observed decomposition can be described stoichiometrically by the equations (m)–(o):

$$C_3H_7CHO = C_3H_8 + CO, \tag{m}$$

$$C_3H_7CHO = \tfrac{1}{2}(C_3H_7)_2 + \tfrac{1}{2}H_2 + CO, \tag{n}$$

$$C_3H_7CHO = C_3H_6 + H_2 + CO. \tag{o}$$

Using mean values for the hydrocarbon yields in Table 24, it can be calculated that the contributions to the decomposition are (m) 54%, (n) 34%, and (o) 12%.

Mass balance

The mole ratios for the products using the mean values in Tables 22–24 are

$$\frac{H}{C} = 2.00 \quad \frac{O}{C} = 0.25.$$

For isobutyraldehyde the values are

$$\frac{H}{C} = 2.00 \quad \frac{O}{C} = 0.25.$$

Thus the agreement is good.

Primary processes

Three separate reactions seem to complete the primary dissociation process [52, 53].

$$C_3H_7CHO + h\nu \rightarrow C_3H_7 + CHO, \tag{P72}$$

$$C_3H_7CHO + h\nu \rightarrow C_3H_8 + CO, \tag{P73}$$

$$C_3H_7CHO + h\nu \rightarrow CH_3 + C_2H_4CHO. \tag{P74}$$

In connection with isobutyraldehyde C_3H_7 refers to the isopropyl radical.

As has been stated above, methane was not present in amounts exceeding 0.01×10^{-8} mole, which suggests that reaction (P74) is not important in the present investigation, compare reaction (55b).

Table 22. Photolysis of isobutyraldehyde in Apparatus II. Determination of the yield of carbon monoxide (CO).

Detector: Thermal conductivity.
Carrier gas: Hydrogen (H_2).
Flow rate of carrier gas: 20 cm^3 min^{-1}.
Stationary phase: Linde Molecular Sieves 5A (30–52 mesh).
Column length: 106 cm.
Column temperature: 45°C.

Pressure of isobutyraldehyde before photolysis mm Hg		Yield of carbon monoxide (Ψ_{CO}) mole × 10^8
29.7		5.2
29.7		5.8
30.0		5.0
30.1		5.3
	Mean value	5.3
11.0		1.5
11.1		2.3
20.8		3.5
20.9		4.0
30.8		5.3
30.9		5.7
31.1		5.6
31.1		5.5
41.0		7.3
41.1		7.0

Blacet and Calvert photolyzed isobutyraldehyde in the presence of iodine and found that reaction (P72) was of importance at all wavelengths investigated (253.7–313 mμ), but reaction (P73) only at the shorter wavelengths [52, 53]. Reaction (P74) was found to be of some importance at short wavelengths. Some doubt has been expressed about the validity of these values, as iodine atoms may selectively deactivate the electronically-excited states involved.

Radical reactions

If the primary process (P74) is neglected, the radical–radical reactions which should be considered are comparatively few,

$$C_3H_7 + C_3H_7 \rightarrow (C_3H_7)_2, \quad (75a)$$

$$C_3H_7 + C_3H_7 \rightarrow C_3H_8 + C_3H_6, \quad (75b)$$

$$CHO + CHO \rightarrow H_2 + 2CO, \quad (54b)$$

$$C_3H_7 + CHO \rightarrow C_3H_7CHO, \quad (76a)$$

$$C_3H_7 + CHO \rightarrow C_3H_8 + CO. \quad (76b)$$

Reactions which are first order with respect to radical concentration are discussed separately on page 65. These reactions seem to be of minor importance.

Table 23. Photolysis of isobutyraldehyde in Apparatus II. Determination of the yield of hydrogen (H_2).

Detector: Thermal conductivity.
Carrier gas: Nitrogen (N_2).
Flow rate of carrier gas: 10 cm^3 min^{-1}.
Stationary phase: Linde Molecular Sieves 5A (30–52 mesh).
Column length: 106 cm.
Column temperature: 30°C.

Pressure of isobutyraldehyde before photolysis mm Hg	Yield of hydrogen (Ψ_{H_2}) mole × 10^8
30.1	1.55
30.1	1.49
30.3	1.57
30.3	1.52
30.4	1.48
Mean value	1.52

Table 24. Photolysis of isobutyraldehyde in Apparatus II. Determination of the yields of propane (C_3H_8), propylene (C_3H_6), and di-isopropyl ($(C_3H_7)_2$).

Detector: Flame ionization.
Carrier gas: Hydrogen (H_2).
Flow rate of carrier gas: 20 cm^3 min^{-1}.
Stationary phase: Perkin-Elmer F (Tetra ethylene glycol dimethyl ether).
Column length: 106 cm.
Column temperature: 22°C.

Pressure of isobutyraldehyde before photolysis mm Hg	Yield of propane ($\Psi_{C_3H_8}$) mole × 10^8	Yield of propylene ($\Psi_{C_3H_6}$) mole × 10^8	Yield of di-isopropyl ($\Psi_{(C_3H_7)_2}$) mole × 10^8	$\frac{\Psi_{C_3H_6}}{\Psi_{C_3H_8}}$	$\frac{\Psi_{(C_3H_7)_2}}{\Psi_{C_3H_8}}$
30.1	2.86	0.66	0.84	0.23	0.29
30.2	2.83	0.63	0.88	0.22	0.31
30.0	2.81	0.60	0.89	0.21	0.32
30.2	2.81	0.58	0.92	0.21	0.33
30.2	2.95	0.58	0.95	0.20	0.32
Mean value	2.85	0.61	0.90	0.21	0.31

The ratio between the rate constants of reactions (75b) and (75a) can be obtained directly from the yields of propylene and di-isopropyl measured experimentally. Using the mean values in Table 24, one obtains

$$\frac{k_{75b}}{k_{75a}} = 0.68. \qquad \{48\}$$

This value is in quite good agreement with that of 0.65 which Kerr and Trotman-Dickenson recently obtained from a low intensity photolysis study of isobutyralde-

hyde [58]. The value $k_{75b}/k_{75a} = 0.63$ was determined by Heller and Gordon from photolysis of di-isopropyl ketone [59]. Riem and Kutschke photolyzed azoisopropane and determined k_{75b}/k_{75a} to be 0.52 [60].

Reaction (54b) was discussed on page 50.

The available data give no information about the relative importance of reactions (76a) and (76b). The parallel with reaction (55b) suggests that (76b) is the important step, pages 50 and 56.

Aldehydes

Reactions which are first order with respect to radical concentration

It has been shown that the most important radical-forming primary process in the photolysis of the aldehydes under investigation is a cleavage into alkyl and formyl radicals:

$$C_nH_{2n+1}CHO + h\nu \rightarrow C_nH_{2n+1} + CHO. \qquad (P77)$$

The reaction of the alkyl radical with the parent molecule is known to proceed mainly in the following manner

$$C_nH_{2n+1} + C_nH_{2n+1}CHO \rightarrow C_nH_{2n+2} + C_nH_{2n+1}CO. \qquad (78)$$

It seems valuable to determine the relative importance of reaction (78) and the reaction describing the recombination of the alkyl radicals

$$C_nH_{2n+1} + C_nH_{2n+1} \rightarrow C_{2n}H_{4n+2}. \qquad (79)$$

The ratio of the rates of reactions (78) and (79) is

$$\frac{r_{78}}{r_{79}} = \frac{k_{78}}{k_{79}} \frac{[C_nH_{2n+1}CHO]}{[C_nH_{2n+1}]}. \qquad \{49\}$$

Assuming that the radical–radical reactions predominate, it is convenient to identify $C_nH_{2n+1}CHO$ with M, and C_nH_{2n+1} with R_1, page 22. From Eq. {37}, one then obtains

$$\frac{r_{78}}{r_{79}} \approx 2^{\frac{1}{2}} \frac{k_{78}}{k_{79}^{\frac{1}{2}}} \left(\frac{\tau}{\psi_{C_nH_{2n+1}}}\right)^{\frac{1}{2}} [C_nH_{2n+1}CHO]. \qquad \{50\}$$

For acetaldehyde, the value of $k_{78}/k_{79}^{\frac{1}{2}}$ has been derived by Ausloos and Steacie from a photolysis study of azomethane-acetaldehyde mixtures [61]. These workers obtained values for this ratio rising from 8.5×10^{-13} to 230.0×10^{-13} cm$^{\frac{3}{2}}$ molecule$^{-\frac{1}{2}}$ sec$^{-\frac{1}{2}}$ as the temperature was increased from 27 to 165°C. For the photolysis of acetaldehyde in Apparatus III, the temperature rise was calculated to be about 45°C, page 28. If 70°C is then taken as the reaction temperature, a value for $k_{78}/k_{79}^{\frac{1}{2}}$ of 30×10^{-13} cm$^{\frac{3}{2}}$ molecule$^{-\frac{1}{2}}$ sec$^{-\frac{1}{2}}$ is obtained from reference [61]. Twice the measured yield of ethane divided by the volume of the reaction vessel gives an estimate of $\psi_{C_nH_{2n+1}}$, in this case this is the amount of methyl radicals consumed in the formation of the products per unit volume. Taking 3×10^{-4} sec as the flash period (Fig. 13), it can be calculated using Eq. {50} that r_{78}/r_{79} for acetaldehyde is

of the order of 0.03 at maximum acetaldehyde pressure. From Eq. {36} it is known that the rate of reaction (78) will increase in relation to that of reaction (79) as the acetaldehyde pressure increases. Such a behaviour has also been found; the ratio between the yields of methane and ethane being increased at higher pressures of acetaldehyde (Fig. 25). An alternative explanation for an increase in the methane–ethane yield ratio would be, however, that the efficiency of the primary dissociation process (P51) decreased in relation to that of (P52) (page 49) as the acetaldehyde pressure increased. This latter explanation receives support from the fact that the value of r_{78}/r_{79} which was calculated is quite low.

The occurrence of reaction (78) among the reactions following the photolysis of acetaldehyde in Apparatus II seems to be negligible as the product ratios were found to remain constant over the entire pressure interval (Fig. 23).

For propionaldehyde and the butyraldehydes the value of $k_{78}/k_{79}^{\frac{1}{2}}$ is of the same magnitude as for acetaldehyde [47, 54, 58]. Under the conditions of the present investigation, reaction (78) seems therefore to be only of minor importance in the photolysis of these aldehydes. This is also supported by the fact that the ratio between the yields of the products from the photolysis of propionaldehyde in Apparatus II remains virtually constant as the propionaldehyde pressure changes (Fig. 24).

The alkyl radicals are known to decompose to form unsaturated hydrocarbons. The following decompositions have been reported:

$$C_2H_5 \rightarrow C_2H_4 + H, \tag{80}$$

$$C_3H_7 \rightarrow C_3H_6 + H, \tag{81}$$

$$C_3H_7 \rightarrow C_2H_4 + CH_3. \tag{82}$$

Reactions (81) and (82) apply both to the *n*-propyl radical and the isopropyl radical. It seems that the rate constants of reactions (80)–(82) are too low to make a contribution from these reactions important in the present investigation [47, 54, 58].

The formyl radical is known to decompose in the following manner:

$$CHO + B \rightarrow CO + H + B, \tag{83}$$

B being a third body. The stability of the formyl radical has recently been discussed [62, 63]. Calvert gives the value $k_{83} = 4.9 \times 10^{-13} \exp(-15300/\boldsymbol{R}T)$ cm^3 mole^{-1} sec^{-1}. It thus seems unlikely that reaction (83) plays an important part in the present investigation.

Quantum yields

The quantum yields for the main products determined in Apparatus III are considerably lower than the corresponding yields obtained from low intensity photolysis. There are two processes which may cause the observed behaviour:

1. Recombination of the radicals to form the aldehyde.
2. Deactivation of the excited states to the ground state.

1. A recombination of the radicals to form the aldehyde cannot be of importance in the photolysis of acetaldehyde as it has been shown that the reaction occurring as a result of a collision between a methyl and a formyl radical principally produced methane and carbon monoxide, reaction (55b), pages 50 and 56. Although there

Table 25. Photolysis of acetaldehyde in Apparatus III. Determination of the quantum yields for the formation of methane (CH_4), and ethane (C_2H_6).

Detector: Flame ionization.
Carrier gas: Hydrogen (H_2).
Flow rate of carrier gas: 20 cm^3 min^{-1}.
Stationary phase: Linde Molecular Sieves 5A (30–52 mesh).
Column length: 106 cm.
Column temperature: 85°C.

Flash	Actinometer decomposition (amount of Fe^{2+} ions produced) Mean value molecules $\times 10^{-15}$	Pressure of acetaldehyde before photolysis mm Hg	Dose absorbed by the sample quanta $\times 10^{-15}$	Absorbed light intensity[a] (I_a) quanta cm^{-3} sec^{-1} $\times 10^{-19}$	Amount of methane found molecules $\times 10^{-15}$	Quantum yield of methane formation (ϕ_{CH_4})	Amount of ethane found molecules $\times 10^{-15}$	Quantum yield of ethane formation ($\phi_{C_2H_6}$)	$\frac{\phi_{CH_4}}{\phi_{C_2H_6}}$
I	595	72	$21._1$	5.7	0.26_2	0.012	0.21_6	0.010	1.2
		151	$42._4$	11.0	0.31_5	0.0074	0.27_1	0.0064	1.2
		271	$72._6$	19.1	0.50_6	0.0070	0.36_6	0.0050	1.4
II	523	44	$11._5$	3.1	0.18_3	0.016	0.17_8	0.015	1.1
		145	$35._8$	9.3	0.29_6	0.0083	0.24_7	0.0069	1.2
		273	$64._2$	16.9	0.39_2	0.0061	0.33_6	0.0052	1.2
III	703	50	$17._6$	4.7	0.26_4	0.015	0.29_4	0.017	0.8_8
		110	$37._3$	9.7	0.31_2	0.0084	0.37_8	0.010	0.8_4
		193	$63._0$	16.5	0.46_7	0.0074	0.43_0	0.0068	1.1
IV	570	38	$10._9$	2.9	0.18_6	0.017	0.20_0	0.018	0.9_4
		108	$29._7$	7.7	0.34_4	0.012	0.25_2	0.0085	1.4
		271	$69._6$	18.3	0.51_6	0.0074	0.38_9	0.0056	1.3
V	525	38	$10._0$	2.7	0.16_5	0.017	0.20_2	0.020	0.8_5
		143	$35._4$	9.2	0.26_2	0.0074	0.22_3	0.0063	1.2
		275	$65._0$	17.1	0.43_8	0.0067	0.31_2	0.0048	1.4
VI	614	72	$21._9$	5.9	0.22_9	0.010	0.25_0	0.011	0.9_1
		139	$40._3$	10.5	0.28_2	0.0070	0.26_2	0.0065	1.1
		187	$53._3$	14.0	0.40_8	0.0077	0.40_8	0.0077	1.0
VII	626	271	$76._5$	20.6	0.55_8	0.0073	0.30_3	0.0040	1.8
		275	$77._6$	20.2	0.53_6	0.0069	0.46_4	0.0060	1.2

[a] Calculated by setting the flash period, τ, equal to 300 μsec (Fig. 13).

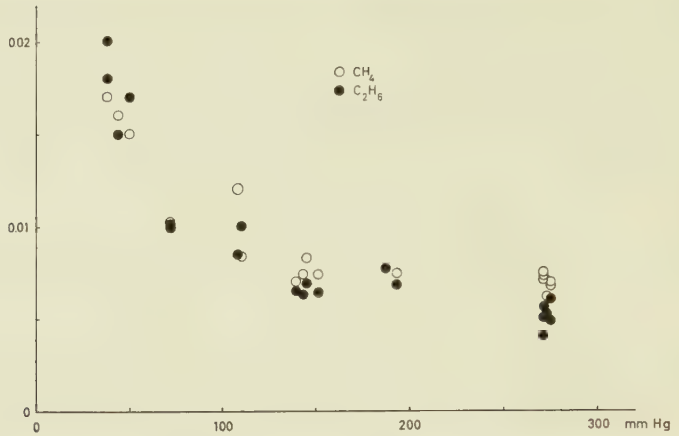

Fig. 25. Photolysis of acetaldehyde in Apparatus III. The quantum yields for the formation of methane and ethane are plotted as a function of the acetaldehyde pressure before photolysis.

is no direct evidence for the assumption that the radical recombination is unimportant in the photolysis of propionaldehyde and the butyraldehydes, the parallel with acetaldehyde suggests that this is the case.

2. Referring to the facts presented in the above discussion, it has been established that a long-lived electronically-excited state is involved in the photolysis of acetaldehyde. The existence of several electronically-excited states in the photolysis of propionaldehyde and the butyraldehydes appears highly probable. However, it seems impossible to obtain any deeper knowledge regarding these states from the available data. For acetaldehyde, the long-lived electronically-excited state has been identified with a triplet state, although no direct evidence for this is available.

It was shown on page 22 that if all reactions of the triplet are first order with respect to triplet concentration, the quantum yield of the decomposition of the triplet molecules will be independent of the intensity of the absorbed light, Eq. {14}. If, on the other hand, the triplet is deactivated to the ground state in triplet–triplet collisions, an intensity dependence would appear, Eq. {13}.

Acetaldehyde.—With the available data a more thorough consideration can only be given to acetaldehyde. For the irradiations with Apparatus III, it seems sufficient to consider reaction (P51) as being the only radical-forming process, page 49. The methyl radicals formed will be consumed in reactions (16) and (55b). On the basis of the above discussion it seems reasonable to assume that the radical–radical reactions predominate. It is then useful to identify CH_3 with R_1 and CHO with R_2 and use the expressions on page 22. From Eq. {20} one obtains

$$\frac{r_{16}}{r_{55b}} = \frac{k_{16}^{\frac{1}{2}} k_{54b}^{\frac{1}{2}}}{k_{55b}}. \qquad \{51\}$$

Table 26. Photolysis of propionaldehyde in Apparatus III. Determination of the quantum yield for the formation of ethane (C_2H_6).

Detector: Flame ionization.
Carrier gas: Hydrogen (H_2).
Flow rate of carrier gas: 20 cm^3 min^{-1}.
Stationary phase: Linde Molecular Sieves 5A (30–52 mesh).
Column length: 106 cm.
Column temperature: 85°C.

Flash	Actinometer decomposition (amount of Fe^{2+} ions produced) Mean value molecules $\times 10^{-15}$	Pressure of propionaldehyde before photolysis mm Hg	Dose absorbed by the sample quanta $\times 10^{-15}$	Absorbed light intensity[a] (I_a) quanta cm^{-3} sec^{-1} $\times 10^{-19}$	Amount of ethane found molecules $\times 10^{-15}$	Quantum yield of ethane formation ($\phi_{C_2H_6}$)
I	655	38	$14._6$	3.9	0.38_6	0.026
		79	$30._2$	7.9	0.75_8	0.025
		160	$58._4$	15.3	1.20	0.021
II	554	38	$12._4$	3.3	0.38_6	0.031
		79	$25._5$	6.6	0.55_2	0.022
		120	$38._0$	10.0	0.69_8	0.018
III	437	38	$9._8$	2.6	0.22_7	0.023
		79	$20._0$	5.2	0.45_4	0.023
		160	$38._7$	10.2	0.83_3	0.022
IV	747	38	$16._7$	4.5	0.44_6	0.027
		38	$16._7$	4.3	0.52_9	0.032
		160	$66._6$	17.5	1.38	0.021

[a] Calculated by setting the flash period, τ, equal to 300 μsec (Fig. 13).

As well as being formed in reaction (55b), methane is also formed in the primary process (P52) and thus

$$\phi_{CH_4} = \phi_{P52} + \frac{k_{55b}}{k_{16}^{\frac{1}{2}}\, k_{54b}^{\frac{1}{2}}}\, \phi_{C_2H_4}, \qquad \{52\}$$

where ϕ_{CH_4} and $\phi_{C_2H_6}$ are the observed quantum yields for the formation of methane and ethane respectively and ϕ_{P52} is the quantum yield of reaction (P52).

The ratio between the quantum yields for the formation of methane and ethane was found to increase with increasing acetaldehyde pressures. In order to explain the pressure dependence of this ratio, it seems plausible to postulate that the quantum yield of the primary process (P52) is constant in the present investigation. Using the values from Table 25, a plot of ϕ_{CH_4} as a function of $\phi_{C_2H_4}$ is given in Fig. 27. The straight line has been drawn according to the method of least squares. From the intercept it is calculated that

$$\phi_{P52} = 0.003. \qquad \{53\}$$

From the slope of the curve one obtains

$$\frac{k_{55b}}{k_{16}^{\frac{1}{2}}\, k_{54b}^{\frac{1}{2}}} = 0.74. \qquad \{54\}$$

Fig. 26. Photolysis of propionaldehyde in Apparatus III. The quantum yield for the formation of ethane is plotted as a function of the propionaldehyde pressure before photolysis.

If an efficient deactivation of the triplet molecule to the ground state in collisions between two such molecules is responsible for the low quantum yield of formation of methane and ethane, Eqs. {27}–{29} can be applied. The constancy of the quantum yield of reaction (P52) suggests that reactions (P52) and (3b) may be identical, i.e. a small portion of the collisions between two triplet molecules result in the formation of a methane and a carbon monoxide molecule, Eq. {27}. An alternative explanation is that reaction (P52) describes a direct decomposition of the excited singlet molecule. For reaction (P51), reactions (4b) and (5b) should then be considered. In the present investigation a variation in the absorbed intensity has been achieved by changing the acetaldehyde pressure, keeping the intensity of the incident light pulse the same. It is then apparent from Eq. {28} that reaction (4b) cannot be of great importance in this case. Assuming reaction (P51) to be identical with reaction (5b), one obtains from Eqs. {19}, {29} and {54}

$$\phi_{C_2H_6} = \frac{1}{2.74} \frac{\gamma^{\frac{1}{2}} k_{5b}}{(2k_{3a} + 2k_{3b})^{\frac{1}{2}}} I_a^{-\frac{1}{2}}. \qquad \{55\}$$

Using the values in Table 25, a plot of the quantum yield of ethane formation as a function of the inverse square root of the intensity is given in Fig. 28. From the best straight line through the origin, the value of

Table 27. Photolysis of *n*-butyraldehyde in Apparatus III. Determination of the quantum yields for the formation of propane (C_3H_8), and ethylene (C_2H_4).

Detector: Flame ionization.
Carrier gas: Hydrogen (H_2).
Flow rate of carrier gas: 20 cm^3 min^{-1}.
Stationary phase: Perkin-Elmer I_0 (Silica Gel).
Column length: 106 cm.
Column temperature: 35°C.

Flash	Actinometer decomposition (amount of Fe^{2+} ions produced) Mean value molecules $\times 10^{-15}$	Pressure of *n*-butyraldehyde before photolysis mm Hg	Dose absorbed by the sample quanta $\times 10^{-15}$	Absorbed light intensity[a] (I_a) quanta cm^{-3} sec^{-1} $\times 10^{-19}$	Amount of propane found molecules $\times 10^{-15}$	Quantum yield of propane formation ($\phi_{C_3H_8}$)	Amount of ethylene found molecules $\times 10^{-15}$	Quantum yield of ethylene formation ($\phi_{C_2H_4}$)	$\frac{\phi_{C_2H_4}}{\phi_{C_3H_8}}$
I	629	40.8	$12._8$	3.4	0.16_3	0.013	0.25_9	0.020	1.5
		41.4	$13._1$	3.4	0.13_3	0.010	0.24_9	0.019	1.9
		41.6	$13._1$	3.4	0.15_5	0.012	0.28_5	0.022	1.8
II	598	40.0	$12._0$	3.2	0.15_0	0.013	0.27_9	0.023	1.8
		40.0	$12._0$	3.1	0.14_8	0.012	0.31_8	0.027	2.3
		40.0	$12._0$	3.1	0.16_7	0.014	0.25_4	0.021	1.5
III	706	41.0	$14._4$	3.9	0.21_0	0.015	0.29_7	0.021	1.4
		40.3	$14._3$	3.7	0.21_4	0.015	0.34_5	0.024	1.6
		40.3	$14._3$	3.8	0.16_7	0.012	0.34_5	0.024	2.0
					Mean value	0.013		0.022	1.8

[a] Calculated by setting the flash period, τ, equal to 300 μsec (Fig. 13).

Table 28. Photolysis of isobutyraldehyde in Apparatus III. Determination of the quantum yield for the formation of propane (C_3H_8).

Detector: Flame ionization.
Carrier gas: Hydrogen (H_2).
Flow rate of carrier gas: 20 cm^3 min^{-1}.
Stationary phase: Perkin-Elmer I_0 (Silica Gel).
Column length: 106 cm.
Column temperature: 35°C.

Flash	Actinometer decomposition (amount of Fe^{2+} ions produced) Mean value molecules $\times 10^{-15}$	Pressure of isobutyraldehyde before photolysis mm Hg	Dose absorbed by the sample quanta $\times 10^{-15}$	Absorbed light intensity[a] (I_a) quanta cm^{-3} sec^{-1} $\times 10^{-19}$	Amount of propane found molecules $\times 10^{-15}$	Quantu yield propa formati ($\phi_{C_3H_8}$)
I	606	40.5	$16._1$	4.3	0.69_1	0.043
		40.7	$16._1$	4.2	0.51_4	0.032
		41.5	$16._6$	4.4	0.62_4	0.038
II	585	40.3	$15._4$	4.1	0.57_3	0.037
		42.5	$16._3$	4.2	0.60_5	0.037
		41.3	$15._7$	4.1	0.54_8	0.035
					Mean value	0.037

[a] Calculated by setting the flash period, τ, equal to 300 μsec (Fig. 13).

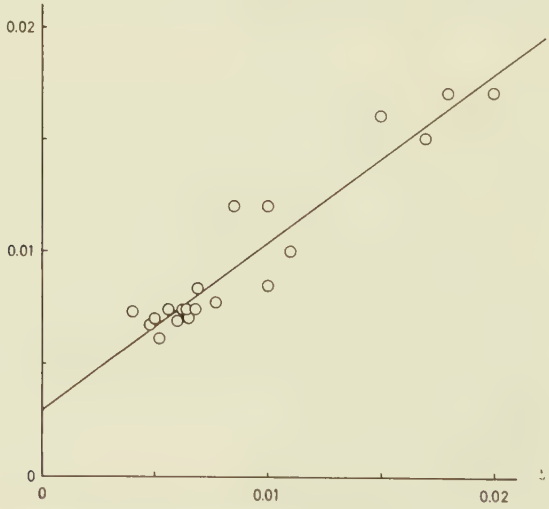

Fig. 27. Photolysis of acetaldehyde in Apparatus III. Plot of ϕ_{CH_4} (the quantum yield of methane) as a function of $\phi_{C_2H_6}$ (the quantum yield of ethane).

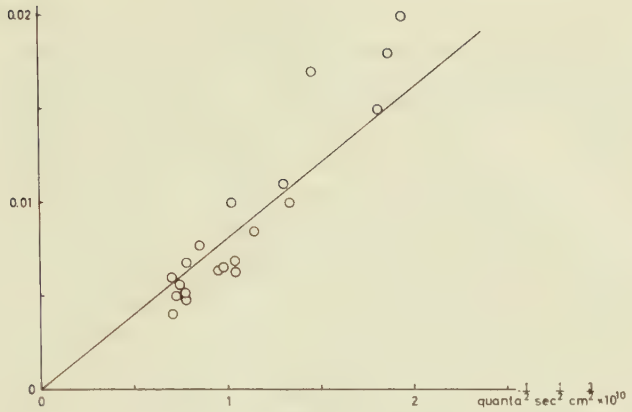

Fig. 28. Photolysis of acetaldehyde in Apparatus III. Plot of $\phi_{C_2H_6}$ (the quantum yield of ethane) as a function of $I_a^{-\frac{1}{2}}$ (the inverse square root of the absorbed intensity).

$$\gamma^{\frac{1}{2}} \frac{k_{5b}}{(k_{3a}+k_{3b})^{\frac{1}{2}}}$$

is calculated to be 33×10^7 molecule$^{\frac{1}{2}}$ sec$^{-\frac{1}{2}}$ cm$^{-\frac{3}{2}}$. The low value of ϕ_{P52} and the low fluorescence quantum yield suggest that γ is close to unity [39]. This leads to the value[1]

$$\frac{k_{5b}}{(k_{3a}+k_{3b})^{\frac{1}{2}}} \approx 3\times10^8 \text{ molecule}^{\frac{1}{2}} \text{ sec}^{-\frac{1}{2}} \text{ cm}^{-\frac{3}{2}}. \qquad \{56\}$$

If it is assumed that a reaction occurs at every triplet–triplet collision, a value of $k_{3a} + k_{3b}$ can be calculated from the classical collision theory. Taking 5 Å as the collision diameter of the triplet, the value of $k_{3a} + k_{3b}$ is calculated to be 2.2×10^{-10} cm^3 molecule^{-1} sec^{-1} at a temperature of 70°C. From Eq. {56} it can then be calculated that k_{5b} will be of the order of 5×10^3 sec^{-1}.

Summary

The vapour phase photolysis of acetone, acetaldehyde, propionaldehyde, *n*-butyraldehyde and isobutyraldehyde has been investigated at very high light intensities.

High intensity flash light sources provided the basis for the experimental investigation. Two of the flash photolysis apparatus, which have been constructed at the Institute of Physical Chemistry, Uppsala, were employed for this purpose.

Analyses for all major products were made on samples which were exposed to unfiltered light in a cylindrical reaction vessel (Apparatus II). In the present case 1800 joules were discharged in this apparatus, giving absorbed intensities of the order

[1] As $k_{3a} \approx k_{3a} + k_{3b}$, $k_{5b}/k_{3a}^{\frac{1}{2}} \approx 3 \times 10^8$ molecule$^{\frac{1}{2}}$ sec$^{-\frac{1}{2}}$ cm$^{-\frac{3}{2}}$.

of 10^{25} quanta sec^{-1} $litre^{-1}$ with a flash period of 10 μsec. The stoichiometry of the products showed that all important constituents were measured.

By using a very intense point-discharge (Apparatus III), quantum yields for the formation of the main products have been determined in parallel light. The samples absorbed light in the absorption band around 280 mμ. Flashes of 100,000 joules, which gave absorbed intensities of the order of 10^{23} quanta sec^{-1} $litre^{-1}$ were used throughout. The absorbed light dose was calculated from a knowledge of the various quantities involved. Thus the spectral distribution of the light emitted from the discharge was determined. The duration of the light pulse from Apparatus III was shown to be strongly dependent of the wavelength of the light isolated, and increases from 30 to 500 μsec when the wavelength is varied from 220 to 500 mμ.

In all cases the samples have been subjected to *one single flash.*

The product yields have been determined by means of gas chromatography using a flame ionization detector or a high sensitivity thermal conductivity detector.

Helium was added in some experiments in order to determine the influence of the reaction temperature on the product yields.

It was found that reactions which are first order with respect to radical concentration could be satisfactorily eliminated. This resulted in a striking simplification of the reaction schemes and has led to new information concerning the primary photochemical mechanisms and the reactions of the formed radicals.

Acetone

Apparatus II. Carbon monoxide and ethane were found to be the major products. Minor products were methane, biacetyl, methyl ethyl ketone, acetaldehyde and hydrogen.

The product yields have been measured as a function of acetone pressure both in the presence and absence of helium, pages 36 and 37.

The addition of helium was found to cause specific changes in the product yields, thus the yield of methane increases whereas the yields of biacetyl and acetaldehyde decreases.

The occurrence of three primary processes has been demonstrated, giving rise to methyl, acetyl, acetonyl radicals and hydrogen atoms. A complete reaction scheme for the reactions of these radicals is presented and discussed.

Apparatus III. The quantum yield for the formation of ethane has been determined as a function of acetone pressure and was found to decrease from 0.017 to 0.009 in the pressure interval 40–170 mm Hg.

The quantum yield determinations show that at high light intensities

> *either* the recombination of radicals to form acetone increases relative to the other reactions
> *or* triplet molecules are effectively deactivated to the ground state in triplet–triplet collisions.

These two possibilities are discussed, page 41.

Aldehydes

Acetaldehyde

Apparatus II. The product yields have been determined as a function of acetaldehyde pressure.

The analytical results can be described by

$$CH_3CHO = CH_4 + CO, \quad (a)$$

$$CH_3CHO = \tfrac{1}{2}C_2H_6 + \tfrac{1}{2}H_2 + CO, \quad (b)$$

$$CH_3CHO = \tfrac{1}{2}CH_3COCH_3 + \tfrac{1}{2}H_2 + \tfrac{1}{2}CO, \quad (c)$$

with the relative importance of (a) 45 %, (b) 41 %, and (c) 14 %.

Apparatus III. The quantum yields for the formation of methane and ethane have been determined as a function of acetaldehyde pressure. In the pressure interval 40–270 mm Hg the quantum yield of methane was found to decrease from 0.017 to 0.007 and that of ethane from 0.020 to 0.005.

Propionaldehyde

Apparatus II. The product yields have been determined as a function of propionaldehyde pressure.

The analytical results can be described by

$$C_2H_5CHO = C_2H_6 + CO, \quad (d)$$

$$C_2H_5CHO = \tfrac{1}{2}C_4H_{10} + \tfrac{1}{2}H_2 + CO, \quad (e)$$

$$C_2H_5CHO = \tfrac{2}{3}C_3H_8 + \tfrac{1}{3}H_2 + CO, \quad (f)$$

$$C_2H_5CHO = C_2H_4 + H_2 + CO, \quad (g)$$

$$C_2H_5CHO = 2CH_4 - H_2 + CO, \quad (h)$$

with the relative importance of (d) 51 %, (e) 37 %, (f) 6.6 %, (g) 4.6 %, and (h) 1.2 %.

Apparatus III. The quantum yield for the formation of ethane has been determined to be about 0.02 and was found to decrease with increasing propionaldehyde pressures.

n-Butyraldehyde

Apparatus II. The product yields have been determined at an *n*-butyraldehyde pressure of 30 mm Hg.

The analytical results can be described by

$$C_3H_7CHO = C_2H_4 + CH_3CHO, \quad (i)$$

$$C_3H_7CHO = C_3H_8 + CO, \quad (j)$$

$$C_3H_7CHO = \tfrac{1}{2}C_6H_{14} + \tfrac{1}{2}H_2 + CO, \quad (k)$$

$$C_3H_7CHO = C_3H_6 + H_2 + CO, \quad (l)$$

with the relative importance of (i) 50 %, (j) 22 %, (k) 25 %, and (l) 2.7 %. Trace quantities of butane and pentane were also found.

Apparatus III. The quantum yields for the formation of propane and ethylene have been determined at 40 mm Hg pressure of *n*-butyraldehyde and found to be 0.013 and 0.022 respectively.

Isobutyraldehyde

Apparatus II. The product yields have been determined at an isobutyraldehyde pressure of 30 mm Hg.

The analytical results can be described by

$$C_3H_7CHO = C_3H_8 + CO, \quad \text{(m)}$$

$$C_3H_7CHO = \tfrac{1}{2}(C_3H_7)_2 + \tfrac{1}{2}H_2 + CO, \quad \text{(n)}$$

$$C_3H_7CHO = C_3H_6 + H_2 + CO, \quad \text{(o)}$$

with the relative importance of (m) 54%, (n) 34%, and (o) 12%.

Apparatus III. The quantum yield for the formation of propane has been determined at 40 mm Hg pressure of isobutyraldehyde and found to be 0.037.

Complete reaction schemes for the reactions between the occurring free radicals are presented and discussed. Some of the information obtained concerning these reactions are as follows.

The reaction between two formyl radicals has been shown to give mainly hydrogen and carbon monoxide (rate constant, k_{54b}).

The predominant reaction as a result of a collision between a methyl and a formyl radical is the formation of methane and carbon monoxide (rate constant, k_{55b}).

The value of $k_{55b}/k_{16}^{\frac{1}{2}}\ k_{54b}^{\frac{1}{2}}$ has been calculated to be 0.74, k_{16} being the rate constant for the combination of two methyl radicals to form ethane.

The ratio between the rate constant of disproportionation and the rate constant of combination of *n*-propyl radicals has been determined to be 0.2.

The ratio between the rate constant of disproportionation and the rate constant of combination of isopropyl radicals has been determined to be 0.68.

The product yields from the photolysis of propionaldehyde agree with the value of 0.15 for the ratio between the rate constant of disproportionation and combination of ethyl radicals, together with the value of 0.06 for the ratio between the rate constant of disproportionation and combination of a methyl and an ethyl radical.

There is indication that long-lived electronically-excited aldehyde molecules are formed which are deactivated to the ground state in collisions between two such molecules.

For acetaldehyde, using Apparatus III, the quantum yield of the primary decomposition into a methane and a carbon monoxide molecule was found to be constant and equal to 0.003. The primary decomposition into a methyl and a formyl radical has been identified with a unimolecular decomposition of an acetaldehyde triplet (rate constant, k_{5b}). The major reaction of the triplet has been postulated to be a deactivation to the ground state in triplet-triplet collisions (rate constant, k_{3a}). The value of $k_{5b}/k_{3a}^{\frac{1}{2}}$ has then been calculated to be of the order of 3×10^{8} molecule$^{\frac{1}{2}}$ sec$^{-\frac{1}{2}}$ cm$^{-\frac{3}{2}}$.

Acknowledgements

The present investigation was carried out at the Institute of Physical Chemistry of the University of Uppsala. It is part of a photochemical research programme at this Institute. The research reported in this document has been sponsored by Air Force Office of Scientific Research of the Air Research and Development Command, United States Air Force, through its European Office and constitutes Technical Note AFOSR TN 59-682.

To the head of the Institute, Professor Stig Claesson, I want to express my sincere gratitude. Professor Claesson introduced me in this field of research and has put the greatest possible facilities at my disposal. His continuous interest and valuable criticism have been very encouraging.

I am indebted to Mr. Bo Malmros for technical assistance and to Dr. David Baird for linguistic suggestions. Thanks are also due to fil. kand. Lave Fischer for valuable discussions during this work.

Institute of Physical Chemistry, University of Uppsala, Uppsala, Sweden.

REFERENCES

1. Noyes, W. A., Jr., and Leighton, P. A., The Photochemistry of Gases. New York, 1941.
2. Davis, W., Chem. Revs. *40*, 201 (1947).
3. Steacie, E. W. R., Atomic and Free Radical Reactions. New York, 1954.
4. Noyes, W. A., Jr., Porter, G. B., and Jolley, J. E., Chem. Revs. *56*, 49 (1956).
5. Khan, M. A., Norrish, R. G. W., and Porter, G., Proc. Roy. Soc. (London) *A 219*, 312 (1953).
6. Mains, G. J., Roebber, J. L., and Rollefson, G. K., J. Phys. Chem. *59*, 733 (1955).
7. Roebber, J. L., Rollefson, G. K., and Pimentel, G. C., J. Am. Chem. Soc. *80*, 255 (1958).
8. Oster, G. K., and Marcus, R. A., J. Chem. Phys. *27*, 472 (1957).
9. Marcus, R. A., Can. J. Chem. *36*, 102 (1958).
10. Heicklen, J., and Noyes, W. A., Jr., J. Am. Chem. Soc. *81*, 3858 (1959).
11. Claesson, S., and Lindqvist, L., Arkiv Kemi *11*, 535 (1957).
12. Claesson, S., and Lindqvist, L., Arkiv Kemi *12*, 1 (1958).
13. Claesson, S., Blixtfotolys och blixtspektroskopi. Svensk Naturvetenskap *13*, 252 (1960).
14. Claesson, S., Nyman, B., and Wettermark, G. To be published.
15. Hatchard, C. G., and Parker, C. A., Proc. Roy. Soc. (London) *A 235*, 518 (1956).
16. Claesson, S., and Wettermark, G., Arkiv Kemi *11*, 561 (1957).
17. Harley, J., Nel, W., and Pretorius, V., Nature *181*, 177 (1958).
18. Thompson, A. E., J. Chromatography *2*, 148 (1959).
19. Dimbat, M., Porter, P. E., and Stross, F. H., Anal. Chem. *28*, 290 (1956).
20. Desty, D. H., Nature *180*, 22 (1957).
21. Nogare, S. D., and Safranski, L. W., Organic Analysis, Vol. 4. New York, 1960.
22. Claesson, S., and Wettermark, G. To be published.
23. Harvey, D., and Chalkley, D. E., Fuel *34*, 191 (1955).
24. Shepp, A., J. Chem. Phys. *24*, 939 (1956).
25. Calvert, J. G., J. Phys. Chem. *61*, 1206 (1957).
26. Ausloos, P., and Steacie, E. W. R., Can. J. Chem. *33*, 47 (1955).
27. Kistiakowsky, G. B., and Roberts, E. K., J. Chem. Phys. *21*, 1637 (1953).
28. Dodd, R. E., and Steacie, E. W. R., Proc. Roy. Soc. (London) *A 223*, 283 (1954).
29. Beckey, H. D., and Groth, W., Z. physik. Chem. (Frankfurt) *20*, 307 (1959).
30. Glazebrook, H. H., and Pearson, T. G., J. Chem. Soc., 567 (1937).
31. Naldrett, S. N., Can. J. Chem. *33*, 750 (1955).
32. Harrison, A. G., and Lossing, F. P., Can. J. Chem. *37*, 1478 (1959).
33. Heicklen, J., J. Am. Chem. Soc. *81*, 3863 (1959).
34. Kaskan, W. E., and Duncan, A. B. F., J. Chem. Phys. *18*, 427 (1950).
35. Herr, D. S., and Noyes, W. A., Jr., J. Am. Chem. Soc. *62*, 2052 (1940).
36. Noyes, W. A., Jr., and Dorfman, L. M., J. Chem. Phys. *16*, 788 (1948).
37. deB. Darwent, B., Allard, M. J., Hartman, M. F., and Lange, L. J., J. Phys. Chem. *64*, 1847 (1960).

38. BERISFORD, R., and LE ROY, D. J., Can. J. Chem. *36*, 983 (1958).
39. MURAD, E., J. Phys. Chem. *64*, 942 (1960).
40. BLACET, F. E., and HELDMAN, J. D., J. Am. Chem. Soc. *64*, 889 (1942).
41. BLACET, F. E., and LEOFFLER, D. E., J. Am. Chem. Soc. *64*, 893 (1942).
42. LOSSING, F. P., Can. J. Chem. *35*, 305 (1957).
43. BLACET, F. E., and BLAEDEL, W. J., J. Am. Chem. Soc. *62*, 3374 (1940).
44. BLAKE, A. R., and KUTSCHKE, K. O., Can. J. Chem. *37*, 1462 (1959).
45. BLACET, F. E., and PITTS, J. N., JR., J. Am. Chem. Soc. *74*, 3382 (1952).
46. SHEPP, A., and KUTSCHKE, K. O., J. Chem. Phys. *26*, 1020 (1957).
47. KERR, J. A., and TROTMAN-DICKENSON, A. F., J. Chem. Soc. 1611 (1960).
48. SMITH, M. J., BEATTY, P. M., PINDER, J. A., and LE ROY, D. J., Can. J. Chem. *33*, 821 (1955).
49. BRINTON, R. K., and STEACIE, E. W. R., Can. J. Chem. *33*, 1840 (1955).
50. JAMES, D. G. L., and STEACIE, E. W. R., Proc. Roy. Soc. (London) *A 244*, 289 (1958).
51. HELLER, C. A., J. Chem. Phys. *28*, 1255 (1958).
52. BLACET, F. E., and CALVERT, J. G., J. Am. Chem. Soc. *73*, 661 (1951).
53. BLACET, F. E., and CALVERT, J. G., J. Am. Chem. Soc. *73*, 667 (1951).
54. KERR, J. A., and TROTMAN-DICKENSON, A. F., Trans. Faraday Soc. *55*, 572 (1959).
55. WHITEWAY, S. G., and MASSON, C. R., J. Chem. Phys. *25*, 233 (1956).
56. CAULE, E. J., and STEACIE, E. W. R., Can. J. Chem. *29*, 103 (1951).
57. MASSON, C. R., J. Am. Chem. Soc. *74*, 4731 (1952).
58. KERR, J. A., and TROTMAN-DICKENSON, A. F., Trans. Faraday Soc. *55*, 921 (1959).
59. HELLER, C. A., and GORDON, A. S., J. Phys. Chem. *62*, 709 (1958).
60. RIEM, R. H., and KUTSCHKE, K. O., Can. J. Chem. *38*, 2332 (1960).
61. AUSLOOS, P., and STEACIE, E. W. R., Can. J. Chem. *33*, 31 (1955).
62. KLEIN, R., and SCHOEN, L. J., J. Chem. Phys. *29*, 953 (1958).
63. CALVERT, J. G., J. Chem. Phys. *29*, 954 (1958).

Tryckt den 27 april 1961

Uppsala 1961. Almqvist & Wiksells Boktryckeri AB